Available online at www.sciencedirect.com
ScienceDirect
Geochimica et Cosmochimica Acta 74 (2010) 7196–7219
Geochimica et Cosmochimica Acta
www.elsevier.com/locate/gca

Corrected version of doi:10.1016/j.gca.2010.09.030 published online with doi:10.1016/j.gca.2011.11.010

Age and geochemistry of volcanic rocks from the Hikurangi and Manihiki oceanic Plateaus

Kaj Hoernle [a,b,*], Folkmar Hauff [a], Paul van den Bogaard [a], Reinhard Werner [a], Nick Mortimer [c], Jörg Geldmacher [d], Dieter Garbe-Schönberg [e], Bryan Davy [f]

[a] *IFM-GEOMAR Leibniz Institute of Marine Sciences, Wischhofstraße 1-3, 24148 Kiel, Germany*
[b] *Department of Earth and Ocean Sciences, University of South Carolina, 701 Sumter Street, Columbia, SC 29208, USA*
[c] *Institute of Geological & Nuclear Sciences, Private Bag 1930, Dunedin, New Zealand*
[d] *IODP-USIO, Texas A&M University, 1000 Discovery Drive, College Station, TX 77845, USA*
[e] *Institute of Geosciences, Christian Albrechts University of Kiel, Ludewig-Meyn-Strasse 10, 24118 Kiel, Germany*
[f] *Institute of Geological & Nuclear Sciences, P.O. Box 30368, Lower Hutt, New Zealand*

Received 8 March 2010; accepted in revised form 13 September 2010; available online 1 October 2010

Abstract

Here we present the first radiometric age data and a comprehensive geochemical data set (including major and trace element and Sr–Nd–Pb–Hf isotope ratios) for samples from the Hikurangi Plateau basement and seamounts on and adjacent to the plateau obtained during the R/V *Sonne* 168 cruise, in addition to age and geochemical data from DSDP Site 317 on the Manihiki Plateau. The $^{40}Ar/^{39}Ar$ age and geochemical data show that the Hikurangi basement lavas (118–96 Ma) have surprisingly similar major and trace element and isotopic characteristics to the Ontong Java Plateau lavas (ca. 120 and 90 Ma), primarily the Kwaimbaita-type composition, whereas the Manihiki DSDP Site 317 lavas (117 Ma) have similar compositions to the Singgalo lavas on the Ontong Java Plateau. Alkalic, incompatible-element-enriched seamount lavas (99–87 Ma and 67 Ma) on the Hikurangi Plateau and adjacent to it (Kiore Seamount), however, were derived from a distinct high time-integrated U/Pb (HIMU)-type mantle source. The seamount lavas are similar in composition to similar-aged alkalic volcanism on New Zealand, indicating a second wide-spread event from a distinct source beginning ca. 20 Ma after the plateau-forming event. Tholeiitic lavas from two Osbourn seamounts on the abyssal plain adjacent to the northeast Hikurangi Plateau margin have extremely depleted incompatible element compositions, but incompatible element characteristics similar to the Hikurangi and Ontong Java Plateau lavas and enriched isotopic compositions intermediate between normal mid-ocean-ridge basalt (N-MORB) and the plateau basement. These younger (~52 Ma) seamounts may have formed through remelting of mafic cumulate rocks associated with the plateau formation. The similarity in age and geochemistry of the Hikurangi, Ontong Java and Manihiki Plateaus suggest derivation from a common mantle source. We propose that the Greater Ontong Java Event, during which ~1% of the Earth's surface was covered with volcanism, resulted from a thermo-chemical superplume/dome that stalled at the transition zone, similar to but larger than the structure imaged presently beneath the South Pacific superswell. The later alkalic volcanism on the Hikurangi Plateau and the Zealandia micro-continent may have been part of a second large-scale volcanic event that may have also triggered the final breakup stage of Gondwana, which resulted in the separation of Zealandia fragments from West Antarctica.

1. INTRODUCTION

The Hikurangi Plateau, located east of the North Island of New Zealand, is a large igneous province (LIP) (Davy and Wood, 1994; Wood and Davy, 1994; Mortimer and

* Corresponding author at: IFM-GEOMAR Leibniz Institute of Marine Sciences, Wischhofstraße 1-3, 24148 Kiel, Germany. Tel.: +49 431 6002642; fax: +49 431 6002924.
E-mail address: khoernle@ifm-geomar.de (K. Hoernle).

0016-7037/$ - see front matter © 2010 Elsevier Ltd. All rights reserved.
doi:10.1016/j.gca.2010.09.030

Parkinson, 1996; Hoernle et al., 2003, 2004) located 3500 km SE of the Ontong Java Plateau and 3000 km SW of the Manihiki Plateau (Figs. 1 and 2). Before the German R/V *Sonne* 168 cruise, igneous rocks from only one site had been successfully recovered from the plateau – at the Rapuhia Scarp on the northern part of the northeastern margin of the plateau. Major and selected trace elements and initial Sr and Nd isotope data from three samples from this site have been previously reported (Mortimer and Parkinson, 1996). One of the major goals of the SO168 cruise was to map and more extensively sample the Hikurangi plateau basement in order to constrain better the age, composition and origin of this LIP, in particular to evaluate possible links to the Ontong Java and Manihiki Plateaus. During the SO168 cruise, igneous rocks were obtained from 31 sites distributed across the entire plateau, including the plateau margin and seamounts on the plateau (Fig. 2).

Two models have been proposed to explain the origin of the igneous rocks of the Hikurangi Plateau: (1) Derivation from a high time-integrated U/Pb (HIMU) mantle plume head that caused the final breakup of the Gondwana supercontinent, i.e. separation of Zealandia, the New Zealand micro-continent (Fig. 1), from Western Antarctica, at ~107 Ma (Storey et al., 1999), and (2) formation contemporaneous with other Pacific plateaus at ca. 120 Ma (Mortimer and Parkinson, 1996), possibly as part of a combined Hikurangi–Manihiki Plateau, which subsequently rifted apart at the Osbourn Trough paleo-spreading center (Fig. 1, Billen and Stock, 2000; Hoernle et al., 2004), or even a combined mega Ontong Java–Manihiki–Hikurangi Plateau (Taylor, 2006). The second model implies that the Hikurangi Plateau first reached the Gondwana (Zealandia) margin after a several thousand kilometer southward journey during the Cretaceous normal superchron (84–121 Ma).

Here we present the first radiometric age and initial Pb and Hf isotopic data, as well as new major and trace element and Sr and Nd isotopic data, from the Hikurangi Plateau basement and the first radiometric age and geochemical data from seamounts on the plateau. In order to facilitate comparison with the Manihiki Plateau, we have also dated two samples and produced a comprehensive geochemical data set (major and trace elements and initial Sr–Nd–Pb–Hf) for seven samples from DSDP Site 317 on the Manihiki High Plateau. The new data confirm that the

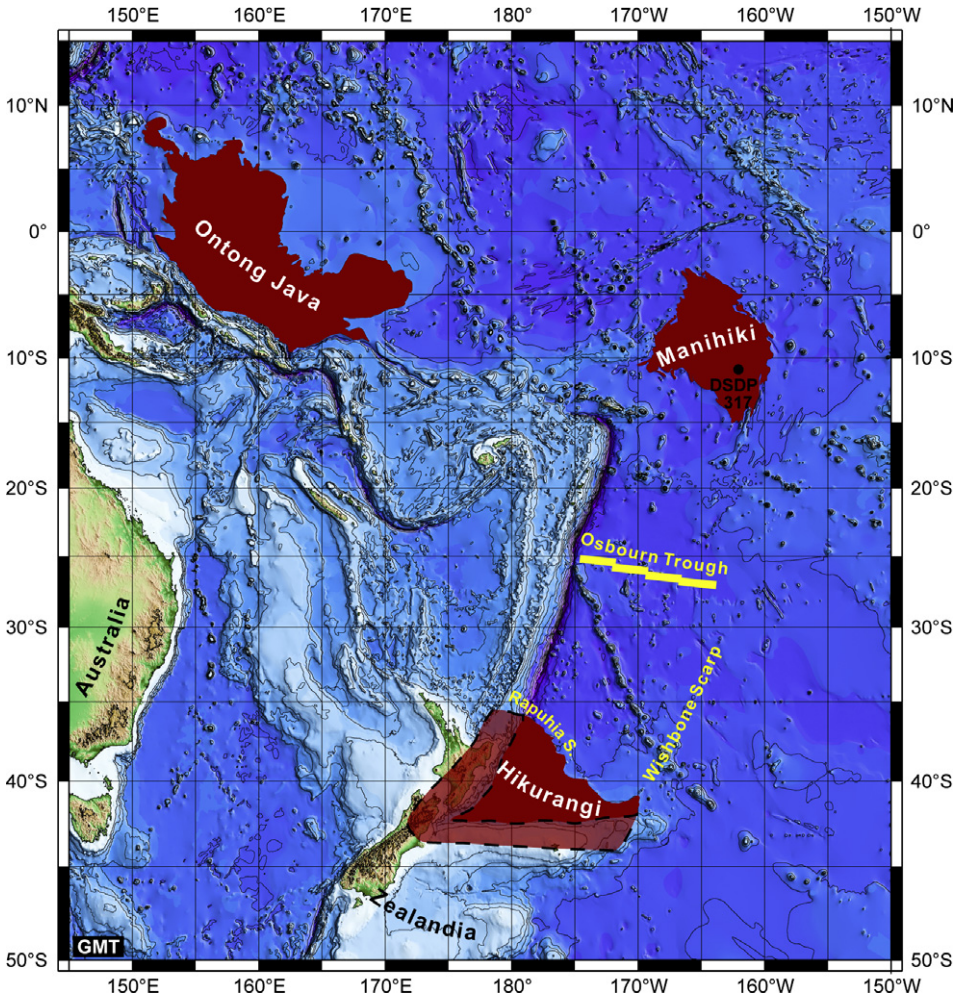

Fig. 1. Overview bathymetric map of the SW Pacific shows the Ontong Java, Manihiki and Hikurangi Plateaus. Base map based on Gebco data set (http://www.gebco.net).

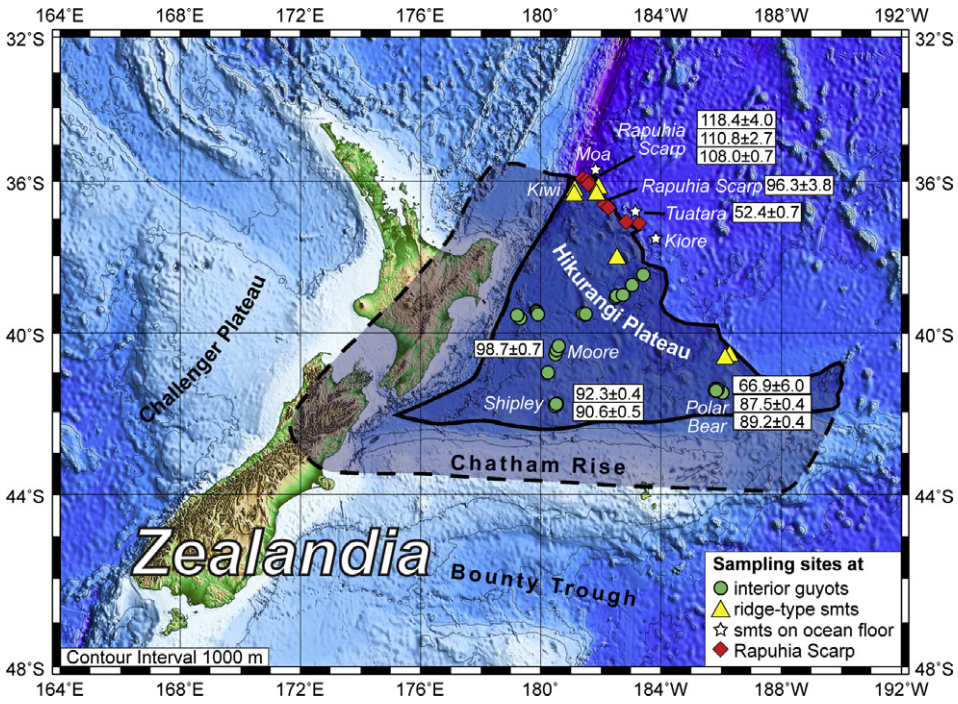

Fig. 2. Map of New Zealand micro-continent Zealandia and the Hikurangi Plateau, also showing dashed traces of the plateau margins subducted beneath the Chatham Rise and New Zealand. Samples from the plateau basement exposed at the Rapuhia Scarp range in age from 118 to 96 Ma, whereas guyot seamounts on the plateau range in age from 99 to 67 Ma. One seamount on the abyssal seafloor adjacent to the NW plateau margin yielded an age of 52 Ma. Ages in millions of years with errors are given in the white boxes. If subducted portions of the Hikurangi Plateau are included, the plateau covered an area of at least 0.8×10^6 km^3 and thus was similar in size to the Manihiki Plateau. Base map from the GEBCO_08 Grid, version 20091120 (http://www.gebco.net).

Hikurangi and Manihiki Plateaus are likely to have formed during the "Greater Ontong Java Event" and were derived from similar mantle sources. This large-scale volcanic event includes not only formation of the Ontong Java, Manihiki and Hikurangi Plateaus, but also volcanism in the Nauru, East Mariana, Lyra and possibly NW Central Pacific Basin in the southwest Pacific and thus covered ~1% of the Earth's surface with submarine volcanism at ca. 122 Ma (Tarduno et al., 1991; Coffin and Eldholm, 1993; Mahoney et al., 1993). Such a massive magmatic event no doubt had a dramatic impact on the life in and chemistry of the Earth's oceans (Larson and Erba, 1999).

The seamounts on the Hikurangi Plateau record a second, later (Late Cretaceous) alkalic magmatic event with HIMU-like geochemical characteristics. Together with similar-aged volcanism on New Zealand which has similar geochemical characteristics, the seamount volcanism may be associated with the final breakup phase of the former Gondwana supercontinent, suggesting that plume-type volcanism was involved in this breakup event (e.g. Weaver et al., 1994; Storey et al., 1999).

2. GEOLOGICAL OVERVIEW, MORPHOLOGY AND ROCK TYPES

The Hikurangi Plateau is triangular in shape, covering ~0.4 million km^2 and generally lies at water depths of 2500–3500 m. Its crustal thickness is not well-constrained but lies between 16 and 23 km and decreases by about one-third where it has been subducted beneath the Chatham Rise (Davy et al., 2008). The western margin of the plateau is actively subducting beneath the North Island of New Zealand and has subducted to a depth of ~65 km thus far (Reyners et al., 2006). Davy and Wood (1994) proposed that at least 150 km of the southern margin of the Hikurangi Plateau was subducted beneath the Chatham Rise in the Cretaceous. Therefore the Hikurangi Plateau must have covered an area of at least 0.8×10^6 km^2, if subducted portions of the plateau are also considered (Fig. 2), making it equal in size to the Manihiki Plateau located ~3000 km to the north.

During the R/V *Sonne* SO168 ZEALANDIA expedition, the northeast plateau margin (Rapuhia Scarp), ~20 seamounts on the Hikurangi Plateau and three seamounts on the abyssal plain adjacent to the NE margin were mapped with a SIMRAD EM120 multi-beam echo-sounding system (Fig. 2) and sampled via dredging (Hoernle et al., 2003, 2004). The SO168 cruise report (Hoernle et al., 2003), which contains sample locations, bathymetric maps of the sampled locations and additional information pertaining to the samples and sampled structures, is available at http://www.ifm-geomar.de/div/projects/zealandia/english/index.html. The northeastern margin of the Hikurangi Plateau rises ~1000 m above the Cretaceous Pacific abyssal plain. The Rapuhia Scarp, a steep (up to 35°) linear slope trending at 135°, forms the northernmost ~150 km of this margin (Fig. 3a). Along the NE margin, the basement steps down to the abyssal plain via a number of terrace-like

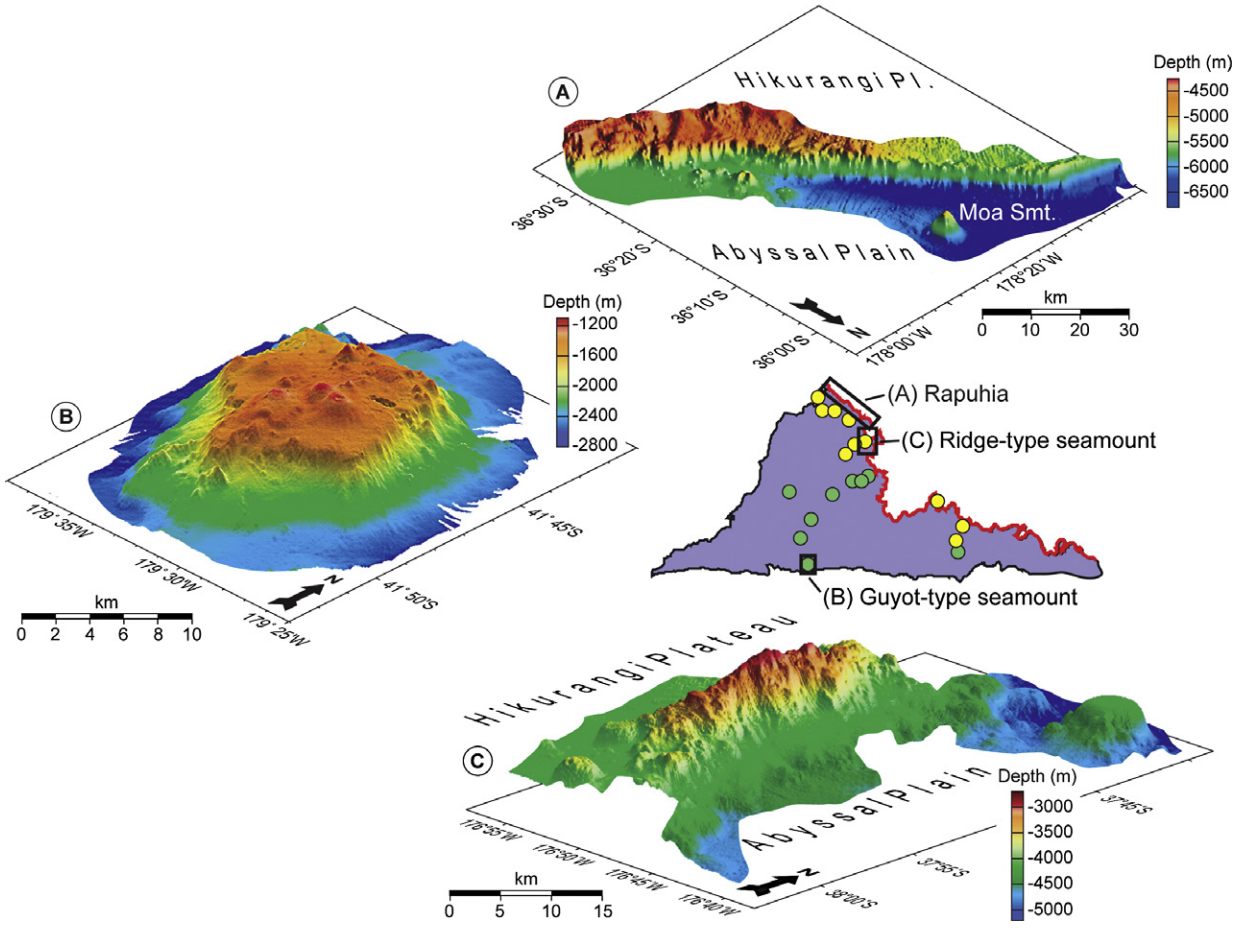

Fig. 3. Morphology of parts of the Hikurangi Plateau obtained during the R/V *Sonne* SO168 ZEALANDIA expedition using a SIMRAD EM120 multi-beam echo-sounding system. (A) Transition from Rapuhia Scarp (northernmost part of the northeast plateau margin exposing the uppermost 1 km of the plateau basement) to region with ridge-type seamounts along the plateau margin; Moa seamount is located on the Cretaceous abyssal plain (Osbourn oceanic crust) adjacent to the scarp. (B) Guyot-type seamount from the southwestern, internal portion of the plateau. (C) Ridge-type seamount located on the northeastern plateau margin southeast of the Rapuhia Scarp shown in (A).

structures (Davy and Wood, 1994; Wood and Davy, 1994), suggestive of step faulting related to rifting (Hoernle et al., 2003). The greatest vertical height of a single scarp was ~800 m, allowing sampling of the uppermost plateau basement. Recovered igneous samples included non- to vesicular basalts, dolerites, gabbros, and abundant volcaniclastic rocks (similar to those from the uppermost Manihiki Plateau; Beiersdorf and Erzinger, 1989).

Two types of large volcanic seamounts occur on the plateau: (1) guyots in the interior of the plateau, characterized by polygonal, steep-sided flanks and relatively flat erosional tops (some of which are >50 km in diameter along their longest axis and ~1 km higher than the plateau basement; Fig. 3b), and (2) ridge-type seamounts near the northeast margin of the plateau (up to 60 km in length, 20 km in width and 2600 m high; Fig. 3c) (Hoernle et al., 2004). Going from the southern boundary of the plateau to the Rapuhia Scarp along the western part of the plateau, the water depth to the top platforms on the guyots and to the base of the guyots increases systematically from ~1600 to 3200 m and ~2600 to 4300 m, respectively, indicating a roughly uniform guyot height of ~1050 m (Hoernle et al., 2004). If sediment thickness is subtracted (Davy et al., 2008), then the guyots have heights of $\geqslant$2 km above the igneous basement. Rock samples from the guyot seamounts range from sandstones and conglomerates to lavas and volcaniclastic breccias. The recovered samples, indicating shallow water to subaerial eruptions and erosion at or above sea level, and the steep-sided, circular or oval, flat-topped morphology are consistent with the guyots being the bases of former island volcanoes, with the flat tops having been formed by erosion of the island to sea level. Late-stage (post-erosional) volcanism occurs on many of the eroded platforms.

The ridge-type seamounts comprise elongated linear features with sharp tops, subparallel to the northeast margin. The elongation of the seamounts is interpreted to result from magmas rising along extensional faults (Hoernle et al., 2004), associated with the breakup of the Hikurangi and Manihiki Plateaus by ca. 115 Ma (Mortimer et al., 2006). The lack of erosional features, such as terraces or platforms, and the higher elevations of some compared to the guyots suggests that these seamounts had extensive late-stage volcanism, post-dating the formation of the

flat-tops on the guyots. All lavas and volcaniclastic rocks dredged from the ridge-type seamounts were highly vesicular, similar to late stage samples from the guyot seamounts. Assuming that there are a minimum of 15 guyot-type seamounts with an average volume before erosion of $\sim$500 km^3 and 15 ridge-type seamounts with an average volume of 1000 km^3, the total seamount volcanism is at least ca. 20,000 km^3, indicating that this was not a small event. This also represents a minimum estimate for the volume of magma involved in the seamount volcanism, since generally most magma forms intrusive rather than extrusive bodies.

Three seamounts on the abyssal plain adjacent to the Rapuhia Scarp were also mapped (e.g. Fig. 3a) and sampled. The northernmost two seamounts Moa and Tuatara (i.e., the Osbourn seamounts) are located on crust that formed at the Osbourn Spreading Center (Worthington et al., 2006). As noted below, Kiore Seamount is compositionally identical to the seamounts on the plateau and thus will be grouped with the Hikurangi seamounts.

Several features are consistent with the northern part of the NE margin representing a rifted margin. These include evidence for step faulting along the Rapuhia Scarp and subparallel faults (represented by the ridge-type seamounts) extending up to 65 km into the plateau along the NE margin. This rifted margin could be associated with the breakup of a formerly combined Hikurangi–Manihiki Plateau (Hoernle et al., 2004; Davy et al., 2008). The lack of a steep scarp or evidence of ridge-type seamounts on the (southern) margin of the Manihiki Plateau similar to the northeast margin of the Hikurangi Plateau suggests highly asymmetric rifting.

3. ANALYTICAL METHODS

Laser $^{40}Ar/^{39}Ar$ analyses were conducted on feldspar and hornblende phenocrysts and microcrystalline basalt matrix chips at the IFM-GEOMAR Geochronology Laboratory. The particles were handpicked from crushed and sieved splits, etched in 5% hydrofluoric acid for 15 min (feldspar), and cleaned using an ultrasonic disintegrator (all samples). See Electronic Annex 1 (EA1) for a description of the analytical methods and EA2 for individual $^{40}Ar/^{39}Ar$ analysis.

Samples selected for geochemistry were first crushed to small pieces, then washed in de-ionized water and carefully handpicked under a binocular microscope. Whole rock powders were then made using an agate mortar and swing mill. Major elements of whole rock samples were determined on fused beads using a Phillips X'Unique PW1480 X-ray fluorescence spectrometer (XRF) equipped with an Rh-tube at IFM-GEOMAR. H_2O and CO_2 were analyzed in an infrared photometer (Rosemount CSA 5003). The XRF data are shown in Electronic Annex 3 (EA3) together with values obtained for the JB-2, JB-3, JA-2 and JR-1 ($N = 10$) standards. The XRF data shown in the plots are normalized to 100% on a volatile free basis. Trace elements were determined by ICP-MS on a VG Plasmaquad PQ1-ICP-MS at the Institute of Geoscience (University of Kiel) after the methods of Garbe-Schönberg (1993). Analytical results for samples and standards (BIR-1, BHVO-1; $N = 4$) are shown in EA3. A subset of samples (marked with an asterisk (*) in EA3) along with BIR-1 and BHVO-2 were analyzed at AcmeLabs by ICPMS using a lithium metaborate/tetraborate fusion technique. For analytical details see www.acmelabs.com.

Sr, Nd and Hf isotope analyses were determined on whole rock powders and Pb on rock chips. Sr and Nd isotope analyses were determined on leached whole rock powders (6 N HCl at 130 °C for 1 h and triple rinsed with ultrapure water thereafter) and Pb on leached rock chips (2 HCl at room temperature for 30 min followed by multiple rinsing in ultrapure water). Powders used for Hf isotope analyses were not leached. The element chromatography followed the methods of Hoernle and Tilton (1991) and Hoernle et al. (2008). Sr–Nd–Pb isotopic ratios were analyzed in static multi-collection mode on the TRITON and MAT262 RPQ2+ thermal ionization mass spectrometers (TIMS) at IFM-GEOMAR. Sr and Nd isotopic ratios are normalized within run to $^{86}Sr/^{88}Sr = 0.1194$ and $^{146}Nd/^{144}Nd = 0.7219$, respectively. All Sr isotope data are reported relative to NBS987 $^{87}Sr/^{86}Sr = 0.710250$ with an external 2σ error of ± 0.000012 ($N = 20$) for the MAT262 and 2σ of ± 0.000009 ($N = 12$) for the TRITON. Similarly the Nd isotope data are reported relative to La Jolla $^{143}Nd/^{144}Nd = 0.511850$ with an external 2σ error of ± 0.00005 ($N = 27$) for the TRITON. NBS981 ($N = 125$; 2003–2006) gave $^{206}Pb/^{204}Pb = 16.898 \pm 0.006$, $^{207}Pb/^{204}Pb = 15.437 \pm 0.007$, $^{208}Pb/^{204}Pb = 36.527 \pm 0.024$ and were corrected for mass bias to our NBS981 double spike values ($N = 69$; 2006–2008) of $^{206}Pb/^{204}Pb = 16.9412 \pm 0.0021$, $^{207}Pb/^{204}Pb = 15.4992 \pm 0.0020$, $^{208}Pb/^{204}Pb = 36.7225 \pm 0.0049$. These values compare well with published double and triple spike data for NBS981 (Baker et al., 1994; Galer and Abouchami, 1998; Thirlwall, 2000, 2002; Baker et al., 2005). Hf chemistry was carried out following the methods of Blichert-Toft et al. (1997) and isotope ratios were measured in static mode on a VG Elemental AXIOM multi-collector magnetic sector inductively coupled plasma mass spectrometer (MC-ICP-MS) at IFM-GEOMAR. Our in-house SPEX Hf ICP standard solution (Lot #9) yields an averaged, JMC 475-normalized value of $^{176}Hf/^{177}Hf = 0.282175 \pm 0.000015$ ($n = 65$). A detailed description of the Hf analytical procedures is found in Geldmacher et al. (2006). Total chemistry blanks were $<$100 pg for Sr, Nd, Hf and Pb and thus considered negligible.

4. RESULTS

4.1. Ar/Ar age data

Basement rocks dredged from the Hikurangi Plateau comprise basalts, gabbros, and dolerites with abundant large phenocrysts of plagioclase feldspar. To avoid the problems of Ar recoil in fine-grained basalt and extensive alteration of the basement whole rock samples, we concentrated on laser fusion of single feldspar crystals, typically several 100 μg in mass after mineral separation. The single-crystal method has the added advantage that older

xenocrysts, crystals contaminated by fluid and melt inclusions, and crystals which have been affected by alteration or thermal resetting can be identified and excluded from the age calculation (Bogaard et al., 1987, 1989; Bogaard, 1995; Gansecki and Mahood, 1998; Giaccio et al., 2009). The best age estimate for such samples is the inverse-variance-weighted mean age derived from a statistically consistent population of single-crystal analyses. A criteria for a single crystal analyses to be included in the best age calculation is that individual crystal ages are within 2σ of the error-weighted mean value. Additional strict criteria for generating an acceptable age is that the measured $^{39}Ar/^{40}Ar$ and $^{36}Ar/^{40}Ar$ ratios of single crystals on inverse isochron plots yield a coherent estimate of the isochron age ($^{40}Ar/^{39}Ar$ intercept), identical within error to the single-crystal mean age, and an initial $^{40}Ar/^{36}Ar$ ratio ($^{40}Ar/^{36}Ar$ intercept) preferably within error of the atmospheric value of 295.5. Fulfillment of these criteria demonstrates that the argon isotope system in the feldspars has not been disturbed and that the calculated single-crystal mean age is accurate. Twelve to 16 single crystals per sample were completely fused and degassed in a single heating step, and their Ar isotope composition analyzed. Results are shown in single-crystal age spectra, probability density graphs, and isochron diagrams (Fig. 4a) and listed in Table 1.

Step-heating was conducted on samples that contain little or no plagioclase phenocrysts or where the plagioclase phenocrysts were too few or too small for single-crystal dating. It was carried out in ca. 20 steps, heating the samples with a de-focused Ar-ion laser beam incrementally to complete fusion and evaporation. Apparent ages (based on an initial $^{40}Ar/^{36}Ar$ ratio of 295.5) and partial ^{39}Ar volumes of the heating steps are plotted on age spectra diagrams. Plateau ages are based on the error-weighted mean of at least three consecutive steps carrying >50% of the total ^{39}Ar released, overlapping in age within 2σ error limits. Step-heating age spectra are shown in Fig. 4b, and results are listed in Table 1.

Statistic validity of single-crystal mean ages, step-heating plateau ages and isochron ages are tested by calculating the MSWD (Mean Square Weighted Deviates; Sum$S/N-1$ for mean ages, Sum$S/N-2$ for isochron ages) and calculating the probability of fit (p), using Chi-Square tables to determine whether the observed scatter of the data around the mean/plateau/isochron is compatible with the measured analytical errors in the isotopic ratios (Baksi, 2003, 2005). MSWD values for single-crystal mean data, step-heating plateau data and isochron data should yield p values >0.05 (95% confidence level). Additional details of the analytical methods and full analytical data are included in EA1. All errors reported in this manuscript are 2σ.

Samples from the deepest parts of the Hikurangi basement, possibly up to 800 m into the plateau basement, were dredged at SO168 Site 34, located at the Rapuhia Scarp and edge of the Kermadec Trench at water depths of between 5400 and 6200 m. Single-crystal analyses of feldspars from a basaltic and a gabbroic sample from this site produced consistent single-crystal ages and best mean ages of 118.4 ± 4.0 Ma (34-4) and 108.0 ± 0.7 Ma (34-11). The single-crystal best mean ages are supported by isotope correlations, yielding isochron ages of 117.2 ± 4.7 Ma (34-4, Initial $= 299.1 \pm 5.5$) and 108.7 ± 0.9 Ma (34-11, Initial $= 285.1 \pm 8.1$) (Fig. 4a).

Single-crystal analyses of feldspars from a dolerite sample at site 34 (34-9), and a dolerite-gabbro sample from ~50 km further southeast along the Rapuhia Scarp (38-3) are more complex. Four out of 14 feldspar crystals of sample 34-9 yield $^{40}Ar/^{39}Ar$ ratios and apparent ages significantly below the bulk population (Fig. 4a). These crystals are suspected to have partially lost their radiogenic ^{40}Ar due to alteration or thermal overprinting, and are therefore excluded from the best age average. The remaining 10 single-crystal ages are consistent within error, and yield a statistically valid mean age of 110.8 ± 2.7 Ma, supported by an isochron age of 110.0 ± 5.0 (Initial $= 299.0 \pm 11.8$).

Two out of 12 feldspar crystals analyzed from dolerite-gabbro 38-3 show the same problem and are excluded from the mean calculation. A third crystal that yields an $^{40}Ar/^{39}Ar$ ratio and apparent age slightly but significantly higher than the bulk population, possibly reflecting excess ^{40}Ar from a contaminant fluid or melt inclusion, is also excluded. The remaining nine single-crystal ages are consistent within error and yield a statistically valid mean age of 96.3 ± 5.0 Ma for dolerite-gabbro 38-3, supported by an isochron age within error of 100.2 ± 8.8 Ma and an initial $^{40}Ar/^{36}Ar$ ratio within error of the atmospheric value (292.1 ± 7.8).

Basalts from internal guyot seamounts on the Hikurangi Plateau (except for Moore Smt.), from seamounts adjacent to the Rapuhia Scarp and from ODP Site 317 on the Manihiki Plateau contain little or no plagioclase phenocrysts or the plagioclase phenocrysts are too few or too small for single-crystal dating. These samples were therefore dated by laser step-heating of mineral separates of feldspar, hornblende or microcrystalline matrix.

Small amounts of plagioclase were extracted from two basalt lava flows drilled at DSDP Site 317 on the Manihiki High Plateau (Schlanger et al., 1976), barely enough (3–4 mg) to carry out two step-heating analyses on each. Fortunately, all of them produced plateaus with only minimal disturbances in the lowest and highest temperature heating steps (Fig. 4b). Unfortunately, results from most heating steps have large error bars, due to generally low signal-to-blank ratios for all Ar isotopes except ^{40}Ar. Two step-heating runs on sample 32R2W54-62 yield statistically valid plateau ages of 117.0 ± 4.7 Ma (W5462fss, 93% ^{39}Ar, 2σ) and 116.4 ± 6.0 Ma (W5462fs2, 89% ^{39}Ar, 2σ), which are identical even within 1σ, and may therefore be combined into a single weighted average (116.8 ± 3.7 Ma), which we consider our best age estimate for Manihiki Plateau sample 32R2W54-62. Two step-heating runs on sample 32R4W125-135 yield statistically valid plateau ages of 117.3 ± 8.0 Ma (W125fss, 100% ^{39}Ar, 2σ) and 115.8 ± 6.7 Ma (W125fs2, 100% ^{39}Ar, 2σ), which are also identical within 1σ, and are therefore combined into a single weighted average (116.4 ± 5.1 Ma), which we consider our best age estimate for Manihiki Plateau sample 32R4W125-135. We note that both DSDP Site 317 sample ages are similar to and within error of the older ages we obtained from Hikurangi basement rocks (samples 34-4 and 34-9).

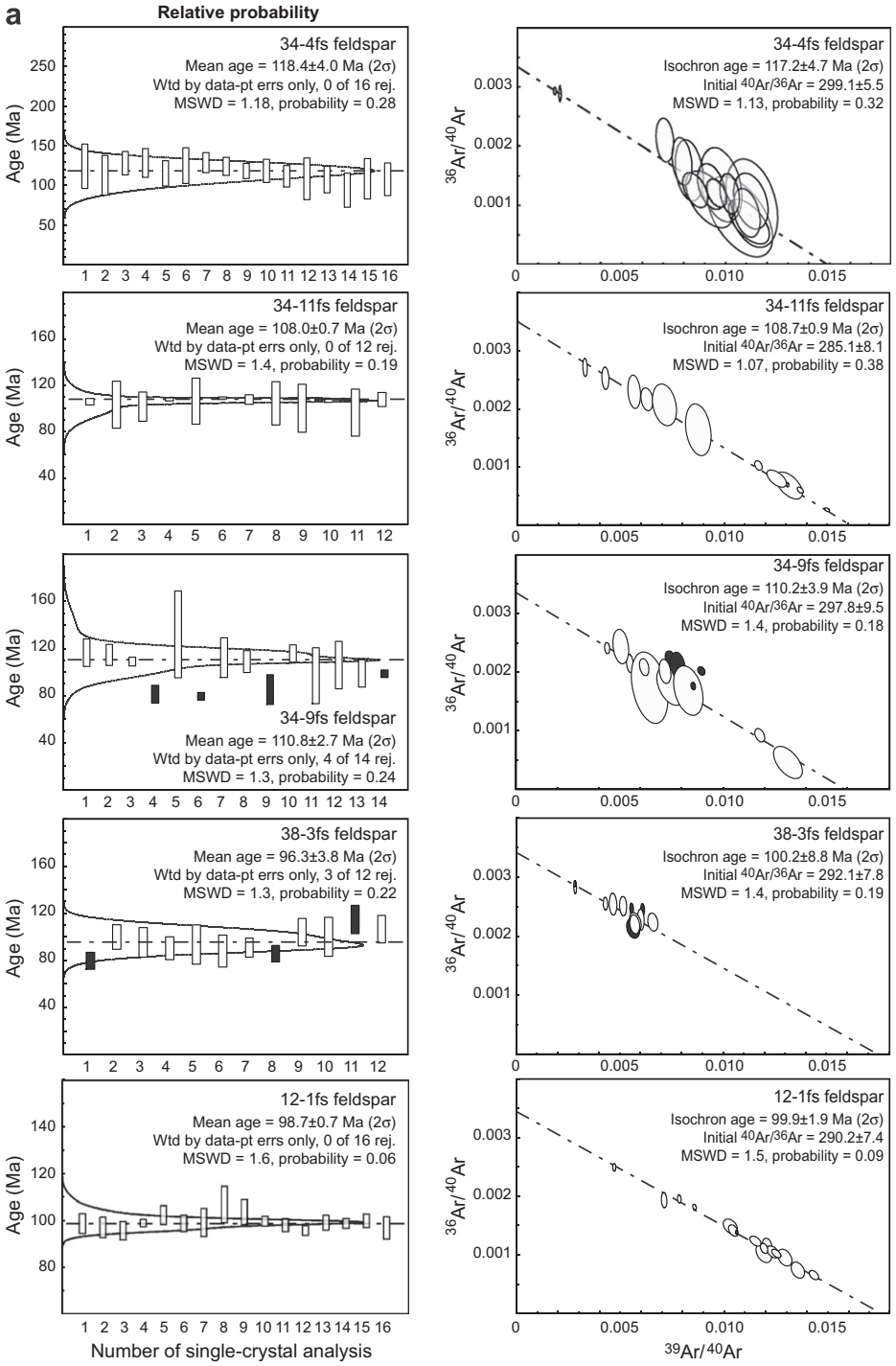

Fig. 4. (a) Single-crystal age spectra and probability density graphs derived from single-crystal apparent ages and assigned errors (left column), and single-crystal inverse isochron diagrams derived from the measured $^{36}Ar/^{40}Ar$ and $^{39}Ar/^{40}Ar$ ratios of the single crystal analyses (right column, $^{39}Ar/^{40}Ar$ ratios normalized to $J = 1.0E-3$). Isochron fit according to York (1969). Error bars and error ellipses are 2σ. Analyses accepted for the mean and isochron calculations are shown in white and rejected crystals in black. Dashed lines represent the mean age with respect to the distribution of data points and relative probability of ages included in the mean age and the isochron in the isotope correlation diagrams. Diagrams generated with the help of Isoplot 3 (Ludwig, 2003). (b) Age spectra derived from laser step-heating apparent ages and assigned errors of hornblende, microcrystalline matrix, and feldspar mineral separates. Error bars are 2σ (excluding J-error). Plateaus are >3 steps, >50% ^{39}Ar, overlapping within 2σ error. Plateau steps are shown in white, rejected steps in black. Dashed line indicates weighted mean of plateau step ages. Diagrams generated with Isoplot 3 (Ludwig, 2003).

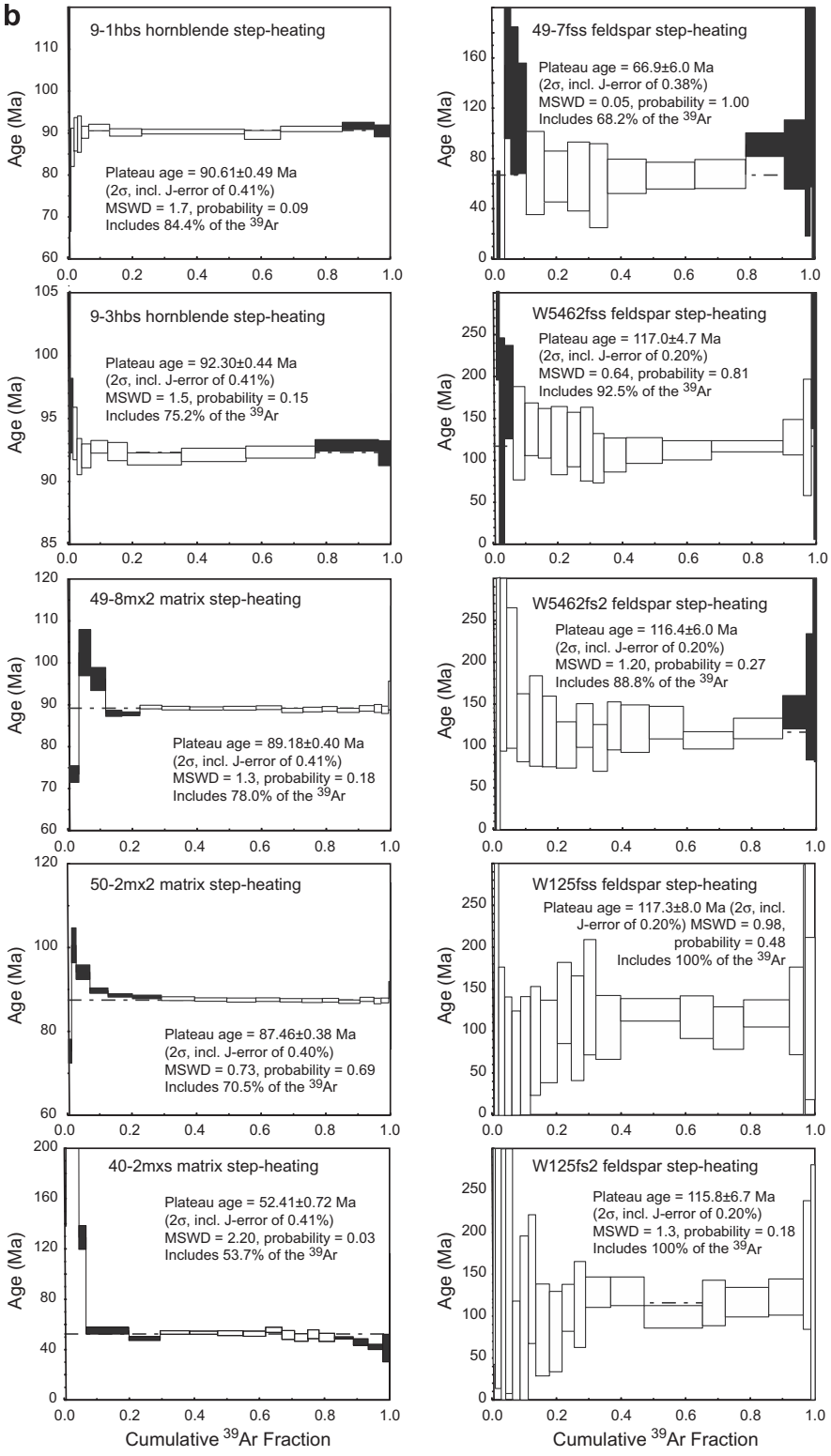

Fig. 4 (*continued*)

Ages were also determined on samples from three large guyot-type seamounts on the Hikurangi plateau. Sixteen feldspars from a lava at the northeast top edge of Moore seamount in the central western part of the plateau yielded consistent single-crystal ages and a best age mean of 98.7 ± 0.7 Ma (12-1), supported by an isochron age within

Table 1
$^{40}Ar/^{39}Ar$ age determinations.

Location and rock type	Sample No.	Lab No.	Material and type of spectrum	Mean age[a] (Ma) $\pm 2\sigma$	MSWD[b]	Probability[c]	No. of crystals analyzed	No. of crystals in mean
Rapuhia Scarp – Hikurangi Plateau								
Basalt	SO168-34-4	34-4fs	Feldspar, single-crystal	118.4 ± 4.0	1.18	0.28	16	16
Gabbro	SO168-34-11	34-11fs	Feldspar, single-crystal	108.0 ± 0.7	1.36	0.19	12	12
Dolerite	SO168-34-9	34-9fs	Feldspar, single-crystal	110.8 ± 2.7	1.30	0.24	14	10
Dolerite-gabbro	SO168-38-3	38-3fs	Feldspar, single-crystal	96.3 ± 3.8	1.30	0.22	12	9
Internal Guyot Seamounts on Hikurangi								
Moore Smt. – basalt	SO168-12-1	12-1fs	Feldspar, single-crystal	98.7 ± 0.7	1.60	0.06	16	16
				Plateau age[a,d] (Ma) $\pm 2\sigma$	MSWD	Probability	Number of steps in plateau	% ^{39}Ar in plateau
Shipley Smt. – basalt	SO168-9-1	9-1hbs	Hornblende, step-heating	90.6 ± 0.5	1.70	0.09	9	84.4
Shipley Smt. – basalt	SO168-9-3	9-3hbs	Hornblende, step-heating	92.3 ± 0.4	1.50	0.15	9	75.2
Polar Bear Smt. – basalt	SO168-49-8	49-8mx2	Matrix, step-heating	89.2 ± 0.4	1.30	0.18	14	78.0
Polar Bear Smt. – basalt	SO168-50-2	50-2mx2	Matrix, step-heating	87.5 ± 0.4	0.73	0.69	11	70.5
Polar Bear Smt. – basalt	SO168-49-7	49-7fss	Feldspar, step-heating	66.9 ± 6.0	0.05	1.00	7	68.2
Seamount adjacent to Rapuhia Scarp – minimum crystal age								
Tuatara Smt. – dolerite	SO168-40-2	40-2mxs	Matrix, step-heating	52.4 ± 0.7	2.20	0.03	9	53.7
Manihiki – basalt	32R2W54-62	W5462fss	Feldspar, step-heating	117.0 ± 4.7	0.64	0.81	13	92.5
Manihiki – basalt	32R2W54-62	W5462fs2	Feldspar, step-heating	116.4 ± 6.0	1.20	0.27	14	88.8
			fss + fs2 weighted mean[e]	116.8 ± 3.7	0.03	0.87		
Manihiki – basalt	34R4W 125-135	W125fss	Feldspar, step-heating	117.3 ± 8.0	0.98	0.48	19	100.0
Manihiki – basalt	34R4W 125-135	W125fs2	Feldspar, step-heating	115.8 ± 6.7	1.30	0.18	20	100.0
			fss + fs2 weighted mean	116.4 ± 5.1	0.08	0.77		

[a] Data points weighted by the inverse variance of assigned errors.
[b] Mean square weighted deviates (Sum$S/N - 1$).
[c] Probability of fit. Probability that assigned errors will yield at least the amount of scatter actually observed.
[d] Number of continuous steps >3, volume ^{39}Ar >50%, ages within 2σ errors (including *J*-error).
[e] Inverse-variance weighted mean of replicate analysis age results.

error (99.9 ± 1.9 Ma) at an initial $^{40}Ar/^{36}Ar$ estimate of 290.2 ± 7.4 (within error of the atmospheric value) (Fig. 4b).

Two separate samples from the southern edge of the erosional platform of Shipley seamount, located in the southwestern part of the plateau, were dated by step-heating analyses of hornblende. Both age spectra show minor disturbances in the high-temperature gas fractions but yielded statistically sound plateaus with ages of 90.6 ± 0.5 Ma (9-1, 84% ^{39}Ar in plateau) and 92.3 ± 0.4 Ma (9-3, 75% ^{39}Ar in plateau) (Fig. 4b).

Two samples from the same dredge haul (49) in a canyon on the SW flank of Polar Bear seamount, located in the eastern central part of the Hikurangi plateau, were analyzed by matrix step-heating (49-8) and feldspar step-heating (49-7). The matrix step-heating spectrum shows minor disturbances in the low-temperature section, probably reflecting ^{39}Ar recoil, but a well-developed 14-step plateau in the mid- to high-temperature section that yields a plateau age of 89.2 ± 0.4 Ma (49-8, 78% ^{39}Ar in plateau). The feldspar step-heating spectrum shows significant disturbances in the low- and high-temperature sections but still an acceptable 7-step plateau in-between with a plateau age of 66.9 ± 6.0 (49-7, 68% ^{39}Ar in plateau). Since post-erosional volcanic cones are located above the canyon, the older sample could be from the shield stage of volcanism and the younger sample from the post-erosional stage.

A basalt sample was collected from the NW flank of Polar Bear seamount (50-2), with no obvious morphological signs of post-erosional volcanism on the platform above the sampling locality. Its step-heating spectrum shows the usual disturbances in the low-temperature steps, again probably reflecting ^{39}Ar recoil of the fine-grained matrix, but yields an 11-step plateau in the mid- to high-temperature section and a plateau age of 87.5 ± 0.4 (71% ^{39}Ar plateau), similar to the older sample from the southwest part of the seamount.

Matrix step-heating of one sample from Tuatara seamount, located on the Osbourn ocean crust, yielded a scattered spectrum with significant disturbances in the low-temperature steps (high apparent ages up to ca. 250 Ma reflecting ^{39}Ar recoil loss?) and in the high-temperature steps (low apparent ages down to ca. 40 Ma from ^{40}Ar loss due to alteration or re-heating?), but also a small 8-step plateau in the mid-temperature heating section comprising 54% of the total ^{39}Ar released and a plateau age of 52.4 ± 0.7 Ma. Scatter and minor disturbances are also present in the plateau, as indicated by a high MSWD (2.2) for $n = 8$, and a probability of fit of 0.03, just below the 0.05 (95% confidence) benchmark. Nevertheless, this sample provides an estimate for the age of Tuatara seamount and a minimum age of the Osbourn ocean crust.

4.2. Major element, trace element and isotope geochemistry

Major and trace element analyses are contained in EA3. As is evident from variable groundmass recrystallization and the presence of phosphates, reflected in high H_2O and P_2O_5 contents and highly variable ratios of mobile to immobile elements (e.g. high K/Nb and U/Pb ratios, indicating K and U uptake from seawater), some samples have undergone extensive seawater alteration. Therefore we concentrate on immobile major and trace elements in this study.

On a diagram of Ti versus V (Fig. 5a), the rocks from the Hikurangi and Manihiki Plateau basements and the Osbourn seamounts have low Ti for their V contents and fall in the N-MORB/Back-arc Basalt field of Shervais (1982), which encompasses rocks with tholeiitic compositions. The seamounts on the Hikurangi Plateau, including Kiore Seamount on the adjacent abyssal floor, have higher Ti for a given V content, plotting within the intra-plate field of Shervais (1982), which consists primarily of alkalic volcanic rocks. The SiO_2 contents of the plateau basement and Osbourn seamounts (47–54 wt%) show a relatively restricted range compared to the Hikurangi seamounts (40–61 wt%), reflecting more silica-undersaturated mafic com-

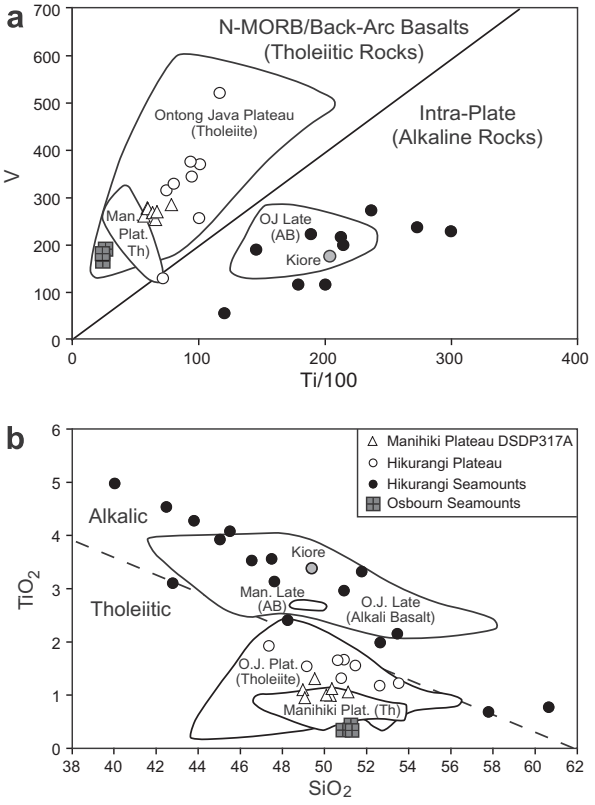

Fig. 5. (a) Ti/100 versus V and (b) SiO_2 versus TiO_2 for volcanic rocks from the (1) Hikurangi, Manihiki and Ontong Java (O.J.) Plateau (Plat.) basement, (2) seamounts on the Hikurangi plateau, and (3) Osbourn (Moa and Tuatara) seamounts on the abyssal seafloor adjacent to the NE plateau margin of the Hikurangi Plateau. Plateau basement and Osbourn seamount volcanic rocks have tholeiitic (Th) compositions, whereas late-stage volcanism from Hikurangi seamount samples (67–99 Ma) and dikes from Ontong Java (ca. 90 Ma) and younger volcanism from Manihiki Plateau (ca. 100 Ma) have alkali basaltic (AB) compositions. Boundaries between "N-MORB/Back-arc Basalts" and "Intra-plate" volcanic rocks from Shervais (1982). Additional data for Ontong Java and Manihiki Plateaus are from GEOROC (http://georoc.mpch-mainz.gwdg.de/georoc/Start.asp).

positions and greater degrees of differentiation (from alkali basalt, basanite and nephelinite to benmoreite and phonotephrite) for the Hikurangi seamounts. Diagrams of SiO_2 versus immobile major and minor elements also show that the Hikurangi and Manihiki basement samples have lower TiO_2 (Fig. 5b) but higher total FeO, V and Sc than the Hikurangi and Kiore seamounts. Kiore seamount sample and Rapuhia Scarp sample 39-2, located below a ridge-type seamount, will henceforth be included in the Hikurangi seamount group, because of their similar compositions (see EA3 and Table 2). The Hikurangi and Manihiki basement and the Osbourn seamount samples fall almost completely within the field for samples from the Ontong Java plateau basement on diagrams of relatively fluid immobile elements such as Ti versus V and SiO_2 versus TiO_2 (Fig. 5).

On multi-element diagrams of immobile incompatible elements (Fig. 6), the Manihiki Plateau samples generally form flat patterns with a pronounced trough at Pb, similar to transitional (T) or enriched (E) mid-ocean-ridge basalts (MORB). Although the Hikurangi basement samples largely overlap with those from Manihiki DSDP Site 317 samples, they extend to lower heavy rare earth element (HREE) and Y abundances, as characterized by higher light (L) and middle (M) to HREE ratios. In addition, Nb and Ta form a slight peak compared to neighboring elements Th and La (and all less incompatible elements), resulting in for example higher (Nb, Ta)/(Th, La, Ce) ratios. Hikurangi basement samples also extend to lower Pb concentrations, probably reflecting mobilization (leaching) of Pb by hydrothermal fluids in the samples with the lowest Pb concentrations. The Osbourn seamount samples display the lowest concentrations of almost all immobile incompatible elements, even compared to N-MORB. These samples also form relatively flat patterns with Pb and slight Zr troughs and Nb and Ta peaks, similar to the Hikurangi samples. Compared with the plateau basement and Osbourn seamount samples, the Hikurangi seamount group samples have higher compositions of almost all incompatible elements (e.g. Ba, Th, Nb, Ta, light REE, Pb, Sr, Zr, Hf, Ti, Y), except for some of the HREEs in some of the samples. They also generally have higher immobile incompatible element ratios, in which the more incompatible element is in the numerator (e.g. Th/Sm, Th/Yb, Nb/Y, Nb/Zr, La/Sm, La/Yb, Zr/Y), than the basement samples. Their incompatible element abundances are typical for volcanic rocks from ocean island basalts (OIBs).

The measured and initial Sr–Nd–Hf–Pb isotopic compositions are presented in Table 2 and Figs. 7–9. Our initial Sr and Nd isotopic compositions from the Hikurangi basement agree well with those from three samples from the basement reported by Mortimer and Parkinson (1996). Hikurangi basement lavas are isotopically distinct from the seamounts. The basement has more enriched mantle (EM)-type isotopic compositions, with more radiogenic initial Sr, Nd (except for one sample) and Hf and less radiogenic Pb isotopic compositions than the seamount lavas. All but one of the Hikurangi basement samples form a group that overlaps the Kwaimbaita/Kroenke lavas at Ontong Java. The distinct sample with the most unradiogenic Nd and Pb isotopic ratios has a composition most similar to the Singgalo lavas from Ontong Java. (It is distinguished in Figs. 7–9 as "Plateau B".) The geochemistry of samples from Kiwi Ridge is indistinguishable from samples from the guyot seamounts (Table 2) and therefore the two types of seamounts will not be distinguished on geochemical diagrams. The Hikurangi seamount samples have high time-integrated $^{238}U/^{204}Pb$ (HIMU)-type trace element and isotopic compositions. The Osbourn seamounts have enriched mid-ocean-ridge basalt (E-MORB)-type isotopic compositions that fall between the Ontong Java, Manihiki and Hikurangi plateau basement and Jurassic-Cretaceous N-MORB.

Our initial $^{87}Sr/^{86}Sr$ and $\varepsilon Nd(t)$ for the Manihiki DSDP Site 317 samples completely overlap with the leached initial compositions obtained by Mahoney (1987) and Mahoney and Spencer (1991), except that one of their samples, from an interval that we did not sample, has higher $\varepsilon Nd(t)$ (5.2) than observed in the samples we analyzed from this site ($\varepsilon Nd(t) = 2.2–3.6$). Our double-spike measured Pb isotope data show slightly less variation than observed in Mahoney and Spencer (1991), and falls completely within the range of their data. The Manihiki DSDP Site 317 samples, in contrast to most of the Hikurangi samples, have compositions similar to the Singgalo lavas at Ontong Java, but are distinct in having slightly lower initial Nd and Hf but higher initial $^{206}Pb/^{204}Pb$ and $^{208}Pb/^{204}Pb$ isotopic ratios.

5. DISCUSSION

5.1. Relationship between Hikurangi, Manihiki and Ontong Java Plateaus

Although no radiometric age data were previously available for the Hikurangi Plateau, the presence of early-middle Campanian to latest Maastrichtian (~70–80 Ma) calcareous rocks recovered from two seamounts (Lewis and Bennett, 1985; Strong, 1994) provide a minimum age for the plateau and some of the seamounts on the plateau. A zircon age of 115 Ma from dacitic lavas from the western flank of the Wishbone Ridge, interpreted to have formed by failed subduction along the Wishbone gravity anomaly, provide a minimum age of 115 Ma for the ocean crust adjacent to the northeast (rifted) Hikurangi margin, constraining the minimum age of the plateau to 115 Ma (Mortimer et al., 2006). Our new $^{40}Ar/^{39}Ar$ age data from feldspar samples from the Hikurangi basement confirm that volcanism began at $\geqslant$118 Ma. Our $^{40}Ar/^{39}Ar$ ages of 116–117 Ma from DSDP Site 317 lavas, from the uppermost portion of the Manihiki Plateau, are consistent with an Aptian age of foraminifera in the sediments overlying the basalts (Bukry, 1976; Mcnulty, 1976; Sliter, 1992). Our ages are also within error of the 117.9 ± 3.5 Ma $^{40}Ar/^{39}Ar$ age determined from a tholeiitic basement sample D2-1 from the Danger Islands Trough, a deep trough that cuts through the center of the Manihiki Plateau (Ingle et al., 2007). Therefore both plateaus could have largely formed contemporaneously with the Ontong Java Plateau at $\geqslant$117 Ma.

Interestingly the relatively large age range of the four samples from the Hikurangi basement (118–96 Ma) falls within the age range observed in tholeiitic samples from

Table 2
Sr–Nd–Hf–Pb isotope data.

Sample	Age (Ma)	$^{206}Pb/^{204}Pb$	±2s	$^{207}Pb/^{204}Pb$	±2s	$^{208}Pb/^{204}Pb$	±2s	$^{238}U/^{204}Pb$	$^{232}Th/^{204}Pb$	$^{206}Pb/^{204}Pb_{(t)}$	$^{207}Pb/^{204}Pb_{(t)}$	$^{208}Pb/^{204}Pb_{(t)}$	$^{87}Sr/^{86}Sr$	±2s	$^{87}Rb/^{86}Sr$	$^{87}Sr/^{86}Sr_{(t)}$	$^{143}Nd/^{144}Nd$	±2s	$^{147}Sm/^{144}Nd$	$^{143}Nd/^{144}Nd_{(t)}$	$eNd_{(t)}$	$^{176}Hf/^{177}Hf$	±2s	$^{176}Lu/^{177}Hf$	$^{176}Hf/^{177}Hf_{(t)}$	$eHf_{(t)}$
Hikurangi Plateau A																										
SO168 DR34-1	110[b]	19.171	2	15.543	1	38.384	4	64.0	48.2	18.07	15.49	38.12	0.703721	6	0.199	0.70341	0.512966	2	0.199	0.51282	6.37					
SO168 DR34-4[a]	118	19.171	13	15.534	11	38.517	26	30[c]	20[c]	18.62	15.51	38.40	0.703742	3		0.70374	0.512954	2	0.203	0.51280	6.06	0.283094	6	0.027	0.283033	11.92
SO168 DR34-9	111	19.217	4	15.528	3	38.292	8	69.6	44.4	18.01	15.47	38.05	0.704123	5	0.406	0.70348	0.512947	3	0.194	0.51281	6.08					
SO168 DR34-11	111												0.704208	4	0.478	0.70347	0.512945	3	0.188	0.51281	6.10					
SO168 DR36-4[a]	110[b]	18.832	13	15.557	10	38.334	26	30[c]	20[c]	18.32	15.53	38.23	0.703796	3		0.70380	0.512926	3	0.190	0.51279	5.70	0.283081	5	0.020	0.283039	11.93
SO168 DR38-1	110[b]	18.712	3	15.594	2	38.450	5	7.8	16.4	18.58	15.59	38.36	0.704725	5	0.721	0.70360	0.512908	2	0.185	0.51277	5.43					
SO168 DR38-3[a]	96	18.533	10	15.511	8	38.132	20	30[c]	20[c]	18.08	15.49	38.04	0.703477	4		0.70348	0.512927	2	0.183	0.51281	5.80	0.283076	4	0.014	0.283049	11.98
SO168 DR38-3													0.703924	5	0.358	0.70344	0.512920	8	0.183	0.51280	5.66					
Hikurangi Plateau B																										
SO168 DR36-1	110[b]	18.737	3	15.540	2	38.314	6	38.3	28.7	18.08	15.51	38.16	0.705308	4	1.01	0.70373	0.512821	2	0.171	0.51271	3.90					
SO168 DR36-1	110[b]	18.578	1	15.531	1	38.149	4	37.6	27.5	17.93	15.50	38.00														
Hikurangi Seamounts																										
SO168 DR9-1	91	20.141	1	15.709	1	39.802	3	51.8	126	19.40	15.67	39.23	0.702907	4	0.072	0.70281	0.512800	3	0.099	0.51274	4.29					
SO168 DR9-3	92	20.190	1	15.722	1	40.067	2	24.3	105	19.84	15.71	39.59	0.702907	4	0.052	0.70284	0.512808	1	0.109	0.51274	4.34	0.282858	6	0.005	0.282848	4.78
SO168 DR12-1	99	20.559	1	15.751	1	40.306	1	24.8	149	20.18	15.73	39.58	0.702873	5	0.158	0.70265	0.512827	2	0.105	0.51276	4.84	0.282807	9	0.006	0.282795	3.06
SO168 DR21-1	90	20.080	1	15.703	0	39.642	1	38.4	132	19.54	15.68	39.06	0.702832	5	0.092	0.70271	0.512883	3	0.122	0.51281	5.63	0.282856	6	0.006	0.282845	4.62
SO168 DR25-1	94	20.223	1	15.731	0	39.837	1	40.1	139	19.63	15.70	39.19	0.702825	5	0.103	0.70269	0.512851	3	0.125	0.51277	5.02					
SO168 DR26-1	94	19.522	1	15.679	0	39.347	1	16.7	63.7	19.28	15.67	39.05	0.702856	5	0.119	0.70270	0.512841	3	0.121	0.51277	4.87					
SO168 DR32-1	94[b]	19.386	1	15.680	1	39.096	1	31[c]	131[c]	18.93	15.66	38.49	0.702796	5	0.081	0.70269	0.512854	3	0.112[c]	0.51279	5.23	0.282896	9	0.006[c]	0.282885	6.14
SO168 DR33-1	94	19.922	1	15.700	1	39.782	1	22.0	128	19.60	15.68	39.18	0.702822	5	0.230	0.70251	0.512811	2	0.111	0.51274	4.39	0.282846	9	0.007	0.282833	4.29
SO168 DR39-2	94	20.173	1	15.718	1	39.999	2	36.5	176	19.64	15.69	39.18	0.703204	5	0.310	0.70279	0.512849	2	0.114	0.51278	5.11					
SO168 DR43-1	52[b]	19.949	1	15.713	1	39.690	1	27.8	117	19.72	15.70	39.39	0.703360	4	0.938	0.70267	0.512816	3	0.121	0.51277	3.98					
SO168 DR47-1	94	19.345	1	15.631	1	38.805	1	41.7	107	18.73	15.60	38.31	0.703076	4	0.084	0.70296	0.512853	2	0.099	0.51279	5.36					
SO168 DR49-1	94	19.957	1	15.720	1	39.668	2	40.7	158	19.36	15.69	38.93	0.703084	5	0.063	0.70300	0.512840	3	0.132	0.51276	4.72					
SO168 DR49-7	67	19.669	1	15.706	1	39.481	1	13.1	93.6	19.53	15.70	39.17	0.703026	5	0.062	0.70297	0.512858	3	0.103	0.51281	5.10	0.282820	4	0.010	0.282807	2.75
SO168 DR49-8	89	20.785	1	15.790	1	40.227	3	33.6	158	20.32	15.77	39.53	0.703325	5	0.222	0.70304	0.512778	3	0.084	0.51273	4.01					
SO168 DR50-2	88	20.682	1	15.791	1	40.253	1	42.4	167	20.10	15.76	39.53	0.703657	5	0.479	0.70306	0.512796	3	0.090	0.51274	4.27					
Osbourn Seamounts																										
SO168 DR35-1	52[b]	18.568	1	15.579	1	38.208	3	12.5	50.4	18.55	15.58	38.19	0.702887	4	0.053	0.70285	0.513039	3	0.201	0.51297	7.79	0.283155	9	0.039	0.283116	13.33
SO168 DR40-1	52[b]												0.703553	5	0.516	0.70317	0.513010	4	0.225	0.51293	7.07	0.283186	4	0.050	0.283136	14.05
SO168 DR40-2	52	22.038	7	15.726	5	38.438	13	352	39.5	19.19	15.59	38.34	0.703553	5	0.460	0.70321	0.513067	3	0.226	0.51299	8.18					
Manihiki DSDP Site 317A																										
31R2W 73-83	117	18.228	2	15.479	2	38.340	5	9.30	42.5	18.06	15.47	38.09	0.704096	5	0.031	0.70405	0.512810	3	0.195	0.51266	3.37					
31R3W 43-50	117	18.341	3	15.493	3	38.344	6	19.3	43.2	17.99	15.48	38.09	0.704019	5	0.006	0.70401	0.512807	2	0.197	0.51266	3.30	0.282988	5	0.030	0.282919	7.94
31R4W 12-23	117	18.257	7	15.478	6	38.341	16	11.4	46.1	18.05	15.47	38.07	0.704003	5	0.010	0.70399	0.512819	3	0.198	0.51267	3.50					
32R2W 54-62	117	18.214	4	15.480	3	38.306	7	9.31	37.6	18.04	15.47	38.09	0.704062	5	0.013	0.70404	0.512826	3	0.200	0.51267	3.62	0.283009	5	0.034	0.282932	8.37
33R4W 81-89	117	18.142	2	15.465	2	38.399	5	11.1	54.8	17.94	15.46	38.08	0.704303	5	0.018	0.70427	0.512740	3	0.184	0.51260	2.19					
34R2W 106-119	117	18.126	2	15.472	2	38.373	4	9.32	48.0	17.96	15.46	38.10	0.704337	5	0.043	0.70427	0.512753	3	0.183	0.51261	2.44	0.282938	5	0.027	0.282875	6.38
34R4W 125-135	116	18.141	2	15.469	2	38.393	5	9.05	45.2	17.98	15.46	38.13	0.704336	5	0.024	0.70430	0.512749	3	0.186	0.51261	2.32					

[a] Pb–Sr isotope analyses carried out on plagioclase; Nd–Hf on whole rock.
[b] Assumed age.
[c] Assumed parent daughter ratios.

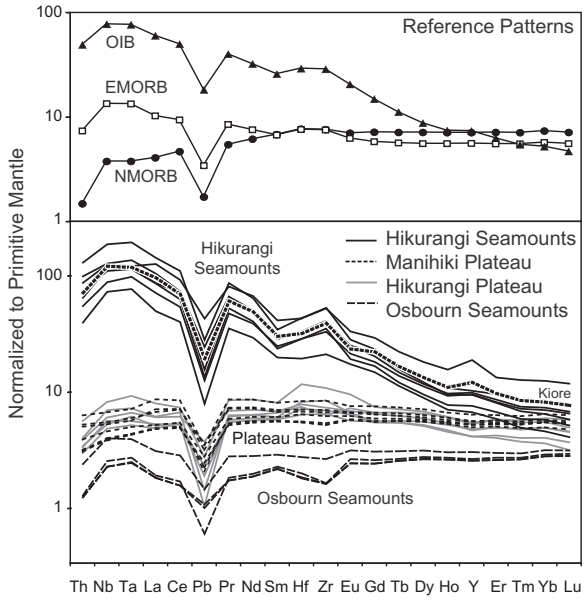

Fig. 6. Representative immobile incompatible trace element diagrams showing increasing highly to moderately incompatible element abundances going from Osbourn seamounts to Hikurangi and Manihiki Plateau basement to Hikurangi seamount samples. Note the extreme depletion in almost all incompatible elements for the Osbourn seamounts, even compared to average normal mid-ocean-ridge basalt (N-MORB). Hikurangi and Manihiki basement samples have patterns similar to average enriched (E)-MORB, whereas the Hikurangi Seamounts have trace element characteristics similar to high time-integrated $^{238}U/^{204}Pb$ (HIMU) ocean island basalt (OIB) from the Cook-Austral island of Mangaia. Average N-MORB, E-MORB and OIB from Sun and McDonough (1989). Kiore seamount sample is denoted separately.

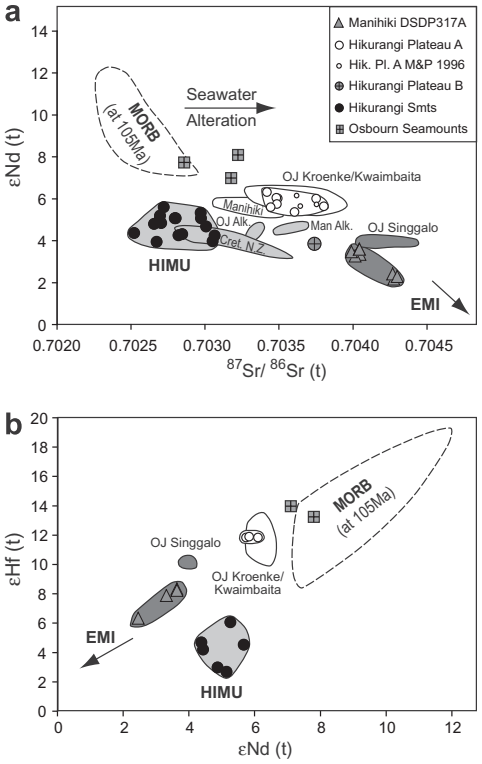

Fig. 7. (a) Initial $^{87}Sr/^{86}Sr$ vs. $\varepsilon Nd(t)$ and (b) $\varepsilon Nd(t)$ vs. $\varepsilon Hf(t)$ isotope diagrams, where (t) denotes the initial isotopic composition at the age (t) at which the sample was formed. Although most Hikurangi basement samples (Hikurangi Plateau A) fall within the field for Kwaimbaita/Kroenke lavas from Ontong Java, one sample (denoted as Hikurangi Plateau B) has lower $^{143}Nd/^{144}Nd$. Manihiki basement samples from DSDP Site 317 have similar $^{87}Sr/^{86}Sr$ but less radiogenic $^{143}Nd/^{144}Nd$ and $^{176}Hf/^{177}Hf$ than the OJ Singgalo samples. Hikurangi seamount lavas have intermediate $^{143}Nd/^{144}Nd$ but less radiogenic $^{176}Hf/^{177}Hf$ compositions compared to plateau basement samples. Cretaceous Mandamus alkaline volcanic rocks (~90–98 Ma) on the South Island of New Zealand (Tappenden, 2003) and Cretaceous basalts on Chatham Island (82–85 Ma; Panter et al., 2006) (referred to collectively as "Cret. N.Z." volcanism) have Sr and Nd isotopic compositions that overlap with the Hikurangi seamount samples. Late-stage (~90 Ma) alkalic dikes on Ontong Java (Sigana alkali basalts on Isabel Island, referred to as OJP Late Stage; Tejada et al., 1996) and alkalic lavas from the Danger Island Troughs on Manihiki have similar Nd but slightly more radiogenic Sr isotope ratios than the Hikurangi seamount lavas, possibly resulting from seawater alteration. Osbourn seamounts (Moa and Tuatara) have isotopic compositions slightly more enriched than Pacific MORB and fall on an extension of the plateau basement array with less radiogenic Sr and more radiogenic Nd and Hf isotopic compositions. Fields for samples from Ontong Java and Danger Island Troughs on Manihiki are based on literature data from Tejeda et al. (1996, 2002, 2004), Mahoney and Spencer (1991) and Ingle et al. (2007). MORB data (excluding data from the Chile Ridge and spreading centers near intersections with seamount chains) are from GEOROC and have been corrected for radiogenic ingrowth over 105 Ma assuming $^{87}Sr/^{86}Sr = 0.005$, $^{147}Sm/^{144}Nd = 0.246$, and $^{176}Lu/^{177}Hf = 0.04$. Mantle acronyms (HIMU and EMI) are after Zindler and Hart (1986). Hikurangi Plateau (Hik. Plat.) A samples from Mortimer and Parkinson (M & P), (1996) are also shown.

Ontong Java (125–85 Ma with peaks at ca. 122 and 91 Ma; e.g. Mahoney et al., 1993; Tejada et al., 1996, 2002) (Fig. 10). Although there can be a problem with Ar recoil in fine-grained basaltic samples, such as primarily dated from Ontong Java, leading to ages significantly younger than the eruption ages, the range in feldspar ages (118–96 Ma) from the Hikurangi basement cannot be explained by Ar recoil. At Site 803D on the NE margin of the Ontong Java Plateau, feldspar ages of 83.7 ± 6.2 and 93.9 ± 2.8 Ma confirm the young whole rock age from this site of 88.2 ± 2.2 Ma (Mahoney et al., 1993). Biostratigraphic dating of nannofossils in sediment layers intercalated with lava flows at Ontong Java give an age range of ca. 120–112 Ma (Sikora and Bergen, 2004), also suggesting that there was volcanism younger than 120 Ma at Ontong Java. The feldspar age data from the Hikurangi basalts provide additional support that igneous activity associated with formation of these plateaus may have been long-lived, lasting $\geqslant 22$ Ma. The cluster of Ontong Java ages at ca. 122 Ma, however, suggests that the later volcanism was likely to be relatively minor with most plateau volcanism occurring at $\geqslant 117$ Ma.

Previous studies have pointed out that the geochemistry of the Hikurangi and Manihiki basement samples are

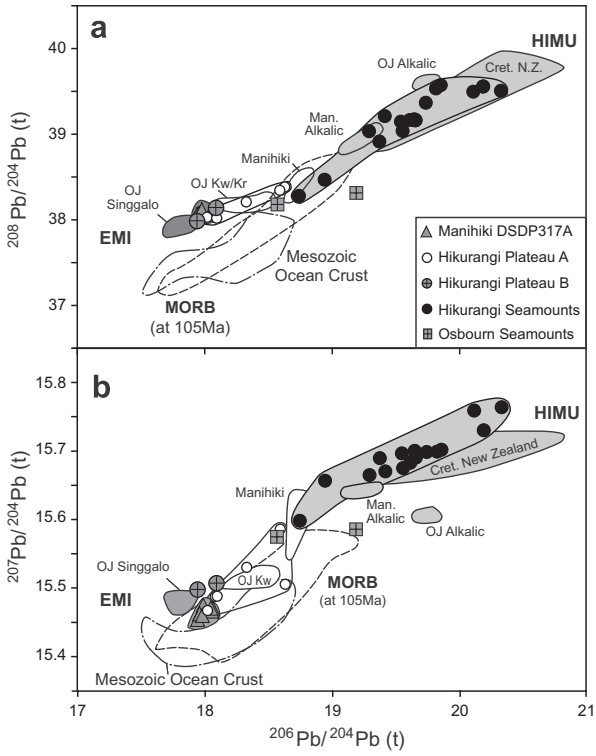

Fig. 8. Initial $^{206}Pb/^{204}Pb$ vs. (a) $^{207}Pb/^{204}Pb$ and (b) $^{208}Pb/^{204}Pb$ isotope correlation diagrams for Hikurangi and Manihiki basement, Hikurangi seamounts and Osbourn seamount samples. The field for Mesozoic Ocean Crust includes data from drilled Mesozoic Ocean Crust reported in Janney and Castillo (1997) and Hauff et al. (2003). For additional data sources and information about the fields shown see caption to Fig. 7.

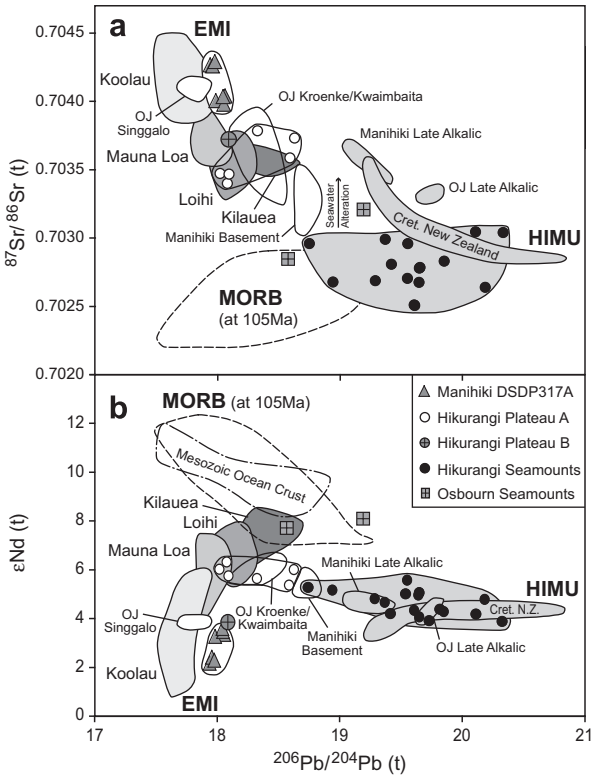

Fig. 9. Initial $^{206}Pb/^{204}Pb$ versus (a) initial $^{87}Sr/^{86}Sr$ and (b) $\varepsilon Nd(t)$ isotope correlation diagrams. Plateau basement lavas from the Hikurangi and Manihiki Plateaus are derived from EM-type sources and are similar in composition to Kwaimbaita/Kroenke and Singgalo lavas on the Ontong Java Plateau. Late-stage alkalic rocks from the three plateaus have more HIMU-like isotopic compositions. Osbourn seamounts have compositions similar to E-MORB and plot on an extension of the plateau basement arrays. Fields for Kilauea, Loihi, Mauna Loa, Koolau (which also contain data from Kahoolawe and Lanai; data from GEOROC) have been corrected for radiogenic ingrowth to 120 Ma, assuming $^{87}Rb/^{86}Sr = 0.015$, $^{147}Sm/^{144}Nd = 0.202$ and $^{238}U/^{204}Pb = 12$ of their sources. Mesozoic Ocean Crust field has been omitted from (a) because of the large range in Sr isotope ratios in seawater altered ocean crust, such that the Sr isotopic composition does not reflect the composition of the upper mantle source of the ocean crust. For additional data sources and information see captions to Figs. 7 and 8.

broadly similar to the composition of Ontong Java lavas (e.g. Mahoney et al., 1993; Mortimer and Parkinson, 1996), but how similar are they in detail? Three different geochemical types of lavas have been identified in tholeiitic lavas on the Ontong Java Plateau: (1) volumetrically dominant Kwaimbaita-type with an isotopic composition similar to the prevalent mantle (PREMA of Zindler and Hart, 1986), (2) mafic Kroenke-type, parental to the isotopically identical Kwaimbaita lavas (Fitton and Godard, 2004; Tejada et al., 2004), and (3) the stratigraphically overlying and volumetrically minor Singgalo-type with a distinct (more EMI-type isotopic) composition (Tejada et al., 2002, 2004). The Hikurangi basement samples (excluding sample DR36-1) have similar immobile element abundances and characteristics, as reflected in the similar and overlapping patterns on multi-element diagrams (Fig. 11), to the Kwaimbaita lavas and to lavas from the Nauru and East Mariana basins (Tejada et al., 2002). Ratios of immobile incompatible trace elements overlap the range in the Kwaimbaita and Kroenke lavas, but are distinct from the Singgalo lavas (see Table 3). The major difference in composition is that the Hikurangi lavas have lower HREE abundances and higher middle to heavy REE ratios, which is likely to reflect the presence of residual garnet in the Hikurangi versus Kroenke/Kwaimbaita source. The Sr–Nd–Hf isotopic compositions of the Hikurangi basement samples also almost completely overlap the field for the Kwaimbaita/Kroenke lavas. Pb isotope ratios of the Hikurangi lavas show a slightly larger range but completely overlap the range observed for the Kwaimbaita and Kroenke group lavas. Although this slightly larger range may reflect the effects of alteration on the Pb isotope system, i.e. U-uptake by seawater and possibly leaching of Pb by hydrothermal fluids, the good to excellent correlation of the Hikurangi basement samples on the Pb isotope diagrams ($r^2 = 1.00$ on the uranogenic diagram if sample 34-4 is excluded; $r^2 = 0.96$ on the thorogenic diagram for all samples) suggests that this could also be a source characteristic. In conclusion, the results from the Hikurangi basement further confirm the widespread distribution of the Kwaimbaita composition and provide new support that igneous activity associated

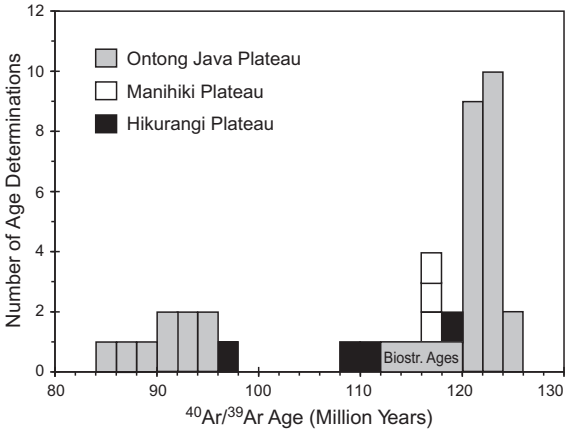

Fig. 10. Compilation of $^{40}Ar/^{39}Ar$ age data from the tholeiitic (basement) parts of the Hikurangi, Manihiki and Ontong Java Plateaus is shown. New $^{40}Ar/^{39}Ar$ feldspar age data from Hikurangi and Manihiki Plateaus show a similar age range to Ontong Java (85–125 my; Mahoney et al., 1993; Tejada et al., 1996, 2002) and previous published Manihiki ages (Ingle et al., 2007). Biostratigraphic (Biostr.) ages of nannofossils in sediment layers intercalated with lava flows at Ontong Java give an age range of 112–120 Ma, suggesting that plateau volcanism continued after 120 Ma (Sikora and Bergen, 2004).

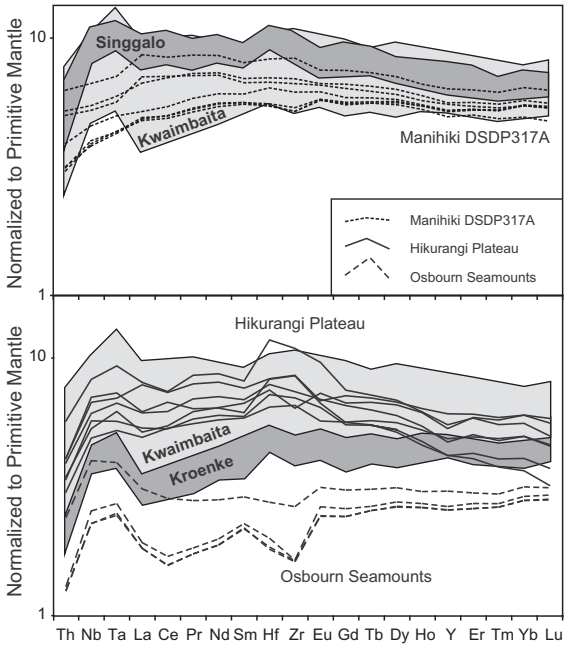

Fig. 11. Incompatible element diagrams comparing lavas from Hikurangi and Manihiki Plateaus and the Osbourn Seamounts with those from Ontong Java (Kroenke, Kwaimbaita and Singgalo groups). See manuscript text for more details about the comparison. Fields for Kroenke, Kwaimbaita and Singgalo rocks based on data from Mahoney et al. (1993), Tejada et al. (2002, 2004) and Fitton and Godard, 2004.

with plateau formation can be derived from a common source over $\geqslant 22$ Ma.

Two distinct groups of lavas have been sampled at the Manihiki Plateau basement: (1) 25 m of cored basalt at DSDP Site 317 (Jackson et al., 1976) and (2) dredge samples from the Danger Island Troughs, which bisect the Manihiki Plateau (Clague, 1976; Ingle et al., 2007). It has been pointed out that the Manihiki DSDP Site 317 samples have similar compositions to Singgalo lavas from Ontong Java (Ingle et al., 2007). Although similar, a detailed comparison shows that the DSDP Site 317 samples generally have lower immobile incompatible element abundances than the Singgalo lavas but have similar incompatible element abundances to the Kwaimbaita lavas (Fig. 11). Furthermore, in contrast to the Ontong Java and Hikurangi basement rocks, the patterns for the DSDP Site 317 lavas do not show the characteristic peak at Nb and Ta relative to La, Ce and Th, reflected, for example, in higher La/(Nb, Ta) ratios (Table 3). The Th/La ratios in the DSDP Site 317 rocks are also lower than in the Singgalo lavas. Finally, although the initial Sr–Nd–Hf–Pb isotopic compositions are broadly similar to the Singgalo lavas, the $^{143}Nd/^{144}Nd$, $^{176}Hf/^{177}Hf$ and $^{207}Pb/^{204}Pb$ isotope ratios are generally lower and the $^{206}Pb/^{204}Pb$ and $^{208}Pb/^{204}Pb$ ratios generally slightly higher than found in the Singgalo lavas, such that the Manihiki DSDP Site 317 samples form distinct fields on Sr–Nd–Hf–Pb isotope correlation diagrams (Figs. 7–9). In conclusion, although their compositions are very similar overall to the Singgalo lavas and to sample DR36-1 from the Hikurangi basement, the Manihiki DSDP Site 317 lavas have distinct compositions compared to all Ontong Java and Hikurangi basement lavas.

The Danger Island Troughs samples from the Manihiki Plateau (Ingle et al., 2007) have distinct trace element and isotopic compositions compared to all Ontong Java and Hikurangi basement samples. Relative to the Kwaimbaita/Kroenke lavas, the most incompatible immobile elements (Th, Nb, Ta, La, Ce) are enriched, the moderately incompatible elements (Pr, Nd, Zr, Hf, Sm), however, are depleted and the HREE and Y overlap or are more depleted in the Danger Island Troughs samples. Ingle et al. (2007) have interpreted the trace element compositions of the tholeiitic Danger Island Troughs samples to result from re-enrichment of a source that was highly depleted through melt extraction and propose that melts from subducted volcaniclastic sediments could have refertilized a highly depleted mantle wedge in a subduction zone. Alkalic lavas also have been recovered from the Danger Island Troughs and seamounts on the plateau (Beiersdorf et al., 1995; Ingle et al., 2007). An $^{40}Ar/^{39}Ar$ age of 99.5 ± 0.7 Ma was obtained on one of the Danger Island Troughs alkalic samples (D3-1; Ingle et al., 2007), indicating that at least some of these lavas post-date the formation of the tholeiitic basement. Accepting a similar range in the isotopic composition of the alkalic volcanism on Manihiki as observed in the Hikurangi seamounts (Hoernle et al., 2008, 2009), then interaction with/addition of small amounts of alkalic melts to older basement lavas derived from a residual or more depleted plateau basement source, similar to the source of the Kroenke/Kwaimbaita/Hikurangi basement lavas, could also explain the higher abundances of the highly incompatible elements. Addition of small amounts of alkalic melts to the basement lavas is also consistent with the less radiogenic Sr, more radiogenic Pb

Table 3
Incompatible element ratios for Ontong Java, Hikurangi and Manihiki Plateaus.

Plateau formation	Ontong Java Kwaimbaita	Ontong Java Kroenke	Ontong Java Kwaim. + Kroenke	Hikurangi Rapuhia	Ontong Java Singgalo	Manihiki DSDP Site 317
La/Sm	1.22–1.48	1.23–1.53	1.22–1.53	1.23–1.64	1.73–1.77	1.36–1.70
La/Ce	0.34–0.38	0.35–0.42	0.34–0.42	0.35–0.42	0.36–0.37	0.37–0.39
La/Yb	1.25–1.76	1.09–1.33	1.09–1.76	1.27–2.14, 2.51[a]	2.24–2.32	1.30–1.99
Ce/Yb	3.60–4.66	3.08–3.34	3.08–4.66	3.51–5.13, 7.13[a]	6.11–6.35	3.45–5.07
La/Nb	0.80–1.09	0.80–0.98	0.80–1.09	0.87–1.16	0.79–0.92	1.13–1.34
La/Zr	0.045–0.056	0.046–0.057	0.045–0.057	0.046–0.058	0.050–0.057	0.053–0.067
La/Th	10.6–13.3	11.2–13.6	10.6–13.6	10.7–14.6	10.0–11.1	9.7–11.8
La/Ta	13.2–15.9	13.5–17.2	13.2–17.2	14.6–19.7	14.5–14.7	18.2–21.9
La/Hf	1.59–2.01	1.61–2.06	1.59–2.06	1.57–2.17	2.17–2.20	1.86–2.41
Nb/Zr	0.051–0.058	0.055–0.060	0.051–0.060	0.047–0.053	0.062–0.063	0.047–0.051

[a] Anomalous value for sample SO168 DR34-11.

and similar Nd isotope ratios of the Danger Island Troughs samples as compared to the Ontong Java and Hikurangi basement rocks (Figs. 7–9).

It has been proposed that the Manihiki and Hikurangi plateaus were once linked and that they rifted apart at the Osbourn Trough (Billen and Stock, 2000; Worthington et al., 2006; Davy et al., 2008) at >115 Ma (Mortimer et al., 2006) and even that both of these plateaus were once connected to the Ontong Java Plateau to form a mega-plateau (Taylor, 2006). Although there is not a direct overlap in the compositions obtained thus far from the Manihiki and Hikurangi plateaus, the isotopic composition of the basement of the two plateaus lie along a common array, consistent with derivation from common sources. The similar ages and the possible derivation from common sources are consistent with these two plateaus having once formed a single plateau. Interestingly the geochemical similarities between the Hikurangi and the Ontong Java Plateau basements is much closer, with most Hikurangi volcanic rocks having similar compositions to the dominant Kwaimbaita type lavas on Ontong Java. In addition, one Hikurangi basement sample has a very similar composition to the minor Singgalo group on Ontong Java. Although not identical in composition, the Manihiki DSDP Site 317 lavas are still quite similar to the Singgalo lavas, also suggesting possible derivation from common sources. The thinner crustal thicknesses of the Hikurangi (16–23 km; Davy et al., 2008) and Manihiki (up to 25 km; Viso et al., 2005) plateaus compared to Ontong Java (up to 30–35 km; Gladczenko et al., 1997) suggest that they may formed through lower degrees of melting near the margin of a possible mega-plateau. Lower degrees of melting are consistent with the steeper HREE element patterns in the Kwaimbaita-type Hikurangi rocks, indicating the presence of residual garnet in the source of the Hikurangi magmas. In conclusion our new age and geochemical data are consistent with the three plateaus having once formed a single mega-plateau but do not require this.

The Hikurangi Plateau has an exposed area of ~0.4 million km^2. If estimates of the portions of the Hikurangi Plateau subducted beneath the North Island of New Zealand and the Chatham Rise are included, the Hikurangi plateau originally had a total area of at least 0.8 million km^2, similar to the Manihiki Plateau. Not considering subducted portions, the Ontong Java Plateau covers an area of ca. 2.0 million km^2. A combined OJMH plateau would have covered an area of at least 3.6 million km^2 and possibly at least 4.4 million km^2 if Manihiki was once twice its present size (Larson et al., 2002) with the volume of igneous rocks forming the combined OJMH plateau and filling the adjacent basins being possibly as high as 100 million km^3 (adding to previous estimates of Coffin and Eldholm (1994) and Fitton et al. (2004)). If contemporaneous volcanism in the Nauru, East Mariana, Lyra and NW Central Pacific Basins, on the Mid-Pacific Mountains and guyots throughout the western Pacific (Larson and Erba, 1999) and the Ontong Java, Manihiki and Hikurangi plateaus (including subducted portions that we can constrain) are considered together, the "Greater Ontong Java Event" may have covered $\geqslant 1\%$ of the Earth's surface with submarine volcanism, requiring a melting anomaly in the mantle of similar size.

5.2. Origin of the Greater Ontong Java Event

A fundamental question concerning Earth evolution is what caused the largest known Phanerozoic igneous event on Earth, which included formation not only of the Ontong Java, Manihiki and Hikurangi Plateaus but also volcanism in the Nauru, East Mariana, NW Central Pacific and Lyra basins and possibly formation of the Mid-Pacific Mountains (120 ± 5 Ma) and guyots throughout the western Pacific (Larson and Erba, 1999). Several recent papers have pointed out the problem of explaining the origin of the Ontong Java Plateau alone (e.g. Ingle and Coffin, 2004; Roberge et al., 2004; Thordason, 2004; Korenaga, 2005), not to mention the rest of the volcanism at ca. 120 Ma. The plume head (Mahoney et al., 1993; Tejada et al., 1996, 2002; Neal et al., 1997), bolide impact (Rogers, 1982; Ingle and Coffin, 2004), perisphere (plate separation) (Anderson et al., 1992) and ridge-centered plume stem (e.g. Mahoney and Spencer, 1991; Ito and Clift, 1998) models cannot adequately explain all the chemical and physical aspects of the plateau (Tejada et al., 2004; Korenaga, 2005). As an alternative to these models, Korenaga (2005) proposes extensive melting of fertile ecologitic material (recycled ocean crust) entrained by passively upwelling upper

mantle peridotite beneath or near a mid-ocean ridge to generate the voluminous submarine volcanism required to form the Ontong Java Plateau.

The major problem with the plume head and bolide impact models is that they should have formed a subaerial rather than a submarine plateau (e.g. Korenaga, 2005; Roberge et al., 2005). On the other hand, it is difficult to explain the large volume and homogeneity of much of the Ontong Java Plateau, as well as the surrounding basins and the Hikurangi and Manihiki Plateau, through a plume-ridge interaction model. A problem with the passive upwelling of eclogite model is that the Ontong Java Plateau lavas have major element compositions consistent with melting of fertile peridotite rather than eclogitic or pyroxenitic sources, excluding near total fusion of the eclogite/pyroxenite (Fitton and Godard, 2004; Herzberg, 2004; Tejada et al., 2004; Herzberg et al., 2007). In addition, it has been shown that the composition of Pacific ocean crust between 130 and 170 Ma has a depleted composition similar to that of modern Pacific N-MORB (Janney and Castillo, 1997; Mahoney et al., 1998; Hauff et al., 2003). Eclogite in the upper mantle (representing recycled ocean crust) may have a similar isotopic composition to the peridotitic MORB source mantle, if recycling times for the ocean crust are short (<100 Ma). If recycling times are longer, the eclogite could evolve radiogenic Pb (or HIMU-type) isotopic compositions as a result of U uptake by seafloor alteration and through preferential Pb loss in subduction zones, both leading to higher U/Pb ratios. The plateau rocks however do not have MORB or HIMU-type isotopic compositions or lie on a mixing array between these end-members (Figs. 7–9) and therefore are not consistent with melting upper peridotitic mantle ± eclogite as is required by the eclogite entrainment and bolide impact and perisphere models. Therefore all of the presently proposed models, excluding special circumstances, have significant shortcomings in explaining both the origin of the Ontong Java Plateau and the Greater Ontong Java Event.

As confirmed by our new results from the Hikurangi and Manihiki Plateaus, any model for the origin of the Greater Ontong Java Event (whether or not the plateaus formed as a combined mega-plateau or separate plateaus) must explain the following, in addition to the observations above: (1) the widespread spatial distribution of the Kwaimbaita/Kroenke component in the Ontong Java Plateau and in the surrounding basins (e.g. Nauru, East Mariana and Lyra Basins; e.g. Tejada et al., 2002), in the Hikurangi Plateau basement, and the presence of a similar type component at Manihiki, sampled along the margins of the Danger Island Troughs (Mahoney et al., 1993; Ingle et al., 2007; Hoernle et al., 2008, 2009); (2) the presence of Singgalo-type components on Ontong Java, Manihiki and possibly the Hikurangi Plateau; and (3) the longevity of volcanism on these plateaus (ca. 125–85 Ma, age span of tholeiitic volcanism with Kwaimbaita-type compositions; Mahoney et al., 1993; Tejada et al., 1996, 2002; Chambers et al., 2002; Fitton et al., 2004) with volcanism on each plateau beginning ⩾117 Ma.

The widespread dominance of the strikingly homogeneous Kwaimbaita/Kroenke component at Ontong Java and its surrounding basins, in addition to the Hikurangi and Manihiki Plateaus (Hoernle et al., 2009) implies a well-mixed, large-scale source. The presence of the Singgalo-type component at all three plateaus, however, does indicate some heterogeneity in the source of these plateaus. The similarity in radiogenic isotopic composition of the Kwaimbaita/Kroenke component with lavas from the Hawaiian Volcanoes of Kilauea and Loihi and the Singgalo component with lavas from Mauna Loa and Koolau (Fig. 9) places important constraints on the origin of these components (e.g. Tejada et al., 2002, 2004). The Hawaiian-Emperor volcanic chain is considered the best example of mantle plume volcanism on Earth. The high $^{3}He/^{4}He$ ratios for Hawaiian volcanoes, including Loihi, Kilauea and Mauna Loa Volcanoes (e.g. Kurz et al., 1983; Farley and Neroda, 1998), and recent geophysical studies (e.g. Montelli et al., 2004, 2006; Wolfe et al., 2009) both support a lower mantle origin for the Hawaiian plume. The similarity in isotope geochemistry between the plateau basements and the Hawaiian hotspot lavas therefore supports a similar (deeper mantle) origin for the Greater Ontong Java Event (e.g. Tejada et al., 2004). Isotopic modeling suggests that the Kwaimbaita/Kroenke and Singgalo components, and by analogy the Hawaiian array (at least the dominant Loa array), could be derived from primitive mantle that was slightly fractionated (e.g. through a small amount of partial melting of ⩽1%) 3–4 Ga ago and then evolved as a closed system, presumably stored at the core–mantle boundary (D″ layer), until melted to form the Greater Ontong Java Event (Tejada et al., 2004) and Hawaiian volcanism.

It is noteworthy that volcanic rocks with the Singgalo component stratigraphically overlie volcanic rocks with the Kwaimbaita/Kroenke composition in Central Malaita and 1600 km to the north at DSDP Site 807. Lavas with Singgalo-type compositions were also drilled at the top of the Manihiki High Plateau, whereas lavas with more Kwaimbaita/Kroenke-type compositions were dredged from its deeper basement exposed in the Danger Island Troughs (Mahoney and Spencer, 1991; Ingle et al., 2007). These observations suggest that the Singgalo component formed at the end of the main phase of plateau formation. Based on their higher more to less incompatible element ratios, the Singgalo component is likely to have formed by lower degrees of melting of an isotopically-distinct component compared to the Kwaimbaita–Kroenke component (Fitton and Godard, 2004). Therefore, the Singgalo component could be widely distributed in the source of the Ontong Java Event magmas but is swamped by the more dominant Kwaimbaita/Kroenke component at higher degrees of melting during formation of the main part of the plateau. Interestingly at the Hawaiian Islands, there is a systematic trend in geochemistry with distance from the presumed plume center along the Loa and the Kea trends, indicating time-dependent variations in the source (Abouchami et al., 2005). Lavas within the Loa group, for example, range from Kwaimbaita/Kroenke-like compositions at Loihi presently within the shield stage to Singgalo-type lavas at Mauna Loa, which is near the end of the shield stage, and Koolau (and Kahoolawe and Lanai) with even more extreme EMI-type compositions, erupted at the end of the

shield stage. This trend also suggests that more enriched heterogeneities are sampled at lower degrees of melting at later stages of shield volcanism.

Of the existing models, a "superplume" from the core–mantle boundary can best explain (1) the large aerial extent of the Greater Ontong Java Event, covering approximately 1% of the Earth's surface with volcanism, (2) the large volumes of volcanism involved, and (3) the similar radiogenic isotopic composition to Hawaiian volcanism. Larson (1991) noted that the peak in the extensive mid-Cretaceous volcanic activity began just before the Cretaceous normal superchron (121–84 Ma; Gradstein et al., 1994) and therefore proposed that a "superplume" with dimensions of 6000 by 10,000 km, which formed at the core–mantle boundary at ca. 125 Ma, could have affected convection in the outer core, causing the conditions that generated the Cretaceous superchron. He proposed that the superplume was also the source of the extensive mid-Cretaceous magmatism in the Pacific Basin. This is an attractive model in that it provides a link between the extensive volcanism on the surface of the planet and the Cretaceous normal superchron most likely related to processes in the core. Impingement of a superplume with such dimensions on the base of the lithosphere, however, should have caused immense uplift resulting in a large part of the Greater Ontong Java Event being emplaced subaerially, which does not appear to be the case (e.g. Roberge et al., 2005).

As an alternative to a thermal superplume, a thermochemical superplume or dome that stalled in the transition zone (e.g. Davaille et al., 2002; Courtillot et al., 2003; Farnetani and Samuel, 2005) might be able to resolve this, as well as some of the other outstanding problems concerning the origin of this massive mid-Cretaceous volcanic event (Fig. 12). It has been shown that large upwelling plume heads or domes can interact with or even stall at the transition zone and, after cooling for 20–30 Ma or longer, can sink back into the deeper mantle (Farnetani and Samuel, 2005). A thermochemical superplume/dome could conceivably have fed a dense swarm of widely distributed, contemporaneous secondary plumes as it stalled at the transition zone over a 5–10 Ma interval with lower levels of more diffuse activity following over the next 20–30 Ma. Such a structure could be similar to the superplume/dome-like structure imaged beneath the SW Pacific superswell (~3000–4000 km across) that appears to be feeding a variety of seamount groups/chains at the present through secondary plumes (Suetsugu et al., 2009), but somewhat larger in scale (6000–10,000 km), possibly being the initial precursor to the present superplume/dome beneath the SW Pacific as proposed by Larson (1991).

There are a number of possible additional factors as to why this massive volcanic event may have produced so little subaerial volcanism. Rapid mid-Cretaceous spreading rates of 150–200 mm/year (Larson, 1991; Korenaga, 2005) and formation at or near spreading centers (e.g. Mahoney et al., 1993; Taylor, 2006) of multiple smaller mantle upwellings from a stalled plume head/dome would favor wider distribution of volcanism and formation of submarine plateaus. Plume-ridge interaction of the Foundation and Easter plumes (in areas with high present spreading rates)

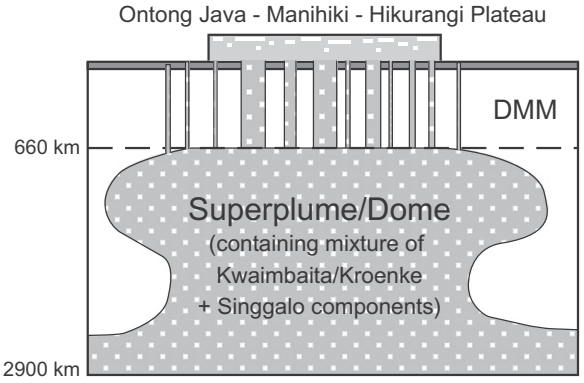

Fig. 12. Model for the formation of the Ontong Java, Hikurangi and Manihiki Plateaus is shown. An upwelling superplume or dome-like structure from the lower mantle may have stalled at the transition zone at approximately 125 Ma. A secondary plume swarm from this stalled superplume may have been responsible for the formation of a combined Ontong Java–Manihiki–Hikurangi super plateau (or separate plateaus) and may also have contributed to volcanism in the surrounding ocean basins. The composition of the upwelling material is heterogeneous with the Kwaimbaita/Kroenke peridotitic component dominating (represented by the gray areas). The minor Singgalo component (represented by the white areas), possibly having a pyroxenetic or eclogitic composition, is only preserved, i.e. not swamped out by the Kwaimbaita/Kroenke component, at relatively low degrees of melting, such as at the end of the plateau stage. The stalled structure could have continued to feed low levels of volcanism for ca. 20–30 Ma, until it sank back into the lower mantle.

forms broad shallow submarine ridges with no or almost no subaerial volcanism. The Galápagos plume located near the Cocos-Nazca Spreading Center (with intermediate spreading rates) forms a shallow submarine plateau with some emergent volcanism. Iceland, which sits on a large submarine plateau, is the only real exception to only localized subaerial volcanism in settings of plume-ridge interaction, but spreading rates in the North Atlantic are low. Therefore a crude correlation appears to exist between the amount of subaerial volcanism in areas where plume volcanism is located on or near a spreading center with faster spreading rates favoring submarine volcanism. Considering that spreading rates in the mid-Cretaceous in the Pacific were up to double the highest present spreading rates, near-ridge plume volcanism on fast-moving lithosphere (as is the case with the Ontong Java, Manihiki and Hikurangi Plateaus; e.g. Mahoney and Spencer, 1991) will favor submarine emplacement.

Recently it has been shown that at least some of the Ontong Java Plateau was subaerial during its formation, based on the presence of accretionary lapilli in a 340 m section of tuff at Site 1184 (Thordason, 2004). Considering the small number of locations where volcanism associated with plateau formation has been reached by drilling (8 Sites on Ontong Java, one on Manihiki and none on Hikurangi), it is likely that additional areas of at least local subaerial volcanism will be found. Another factor that would have prevented the accumulation of volcanism in a given area to

form subaerial edifices is the low viscosity of tholeiitic flood basalts, allowing them to flow large distances and thus spreading out the volcanism. Finally, primarily submarine emplacement of the plateau(s) may also in part result from the lithosphere having obtained a dense (e.g. eclogitic and/or garnet pyroxenitic/peridotitic) root at the same time that the volcanism took place, reflecting addition of frozen plume melts and dense cumulates from these melts to the lithosphere (e.g. Ishikawa et al., 2004; Roberge et al., 2004). This magmatic root may be the source of the low-velocity anomaly observed seismically beneath the Ontong Java Plateau (Richardson et al., 2000). Delamination of parts of this dense eclogitic and/or gt. pyroxenitic/peridotitic root could explain the anomalous (less-than-normal) subsidence of the plateau and help explain younger volcanism on the plateau (Korenaga, 2005). In conclusion, a stalled mantle superplume, plume head or dome, combined with faster Cretaceous spreading rates, high temperature, low-viscosity melts and a magmatic root beneath the plateau(s), could help explain why the Greater Ontong Java Event was largely submarine and why volcanism occurred over an extended (ca. 30 Ma time-span). It could also explain the absence of hotspot tracks associated with the plateau fragments, although it is not clear if the Louisville hotspot track is related to the Ontong Java Plateau.

5.3. Origin of Hikurangi seamount volcanism

The most prominent morphological features on the Hikurangi Plateau are the ~30 large guyot and ridge-type seamounts (Fig. 3b and c). Since these seamounts sit on the top of the plateau, they must be younger than the majority of the basement, which is confirmed by the age data. The ages of the guyots range from 98.7 ± 0.7 to 87.5 ± 0.4 Ma with one age of 66.9 ± 6.0 Ma, possibly representing late-stage (or post-platform, i.e. post-erosional) volcanism. Therefore with the exception of the Rapuhia Scarp sample SO168-38-3 with an age of 96.3 ± 5.0 Ma with a relatively large error that could place its age above 99 Ma, the seamounts are younger than the lavas dated from the basement sampled at the Rapuhia Scarp. Unfortunately no samples from the ridge-type seamount lavas were appropriate for age dating, due to their high vesicularity, extensive alteration, secondary vesicle fill and scarcity of phenocrysts. Since the ridge-type seamounts in part lie directly along the rifted margin, it is likely that a large part of these structures were formed during the initial stages of rifting, or the ridge-like structures would never have formed, because lavas would have flowed over the edge of the rifted margin and pooled on the abyssal seafloor at the base of the rifted margin. The upper part of these seamounts, however, are likely to be younger than the guyot seamounts, since they extend to shallower depths than the erosional platforms forming the tops of the guyots, probably reflecting extensive late-stage volcanism due to reactivation of the rift-related faults along which they initially formed. Minor amounts of late-stage volcanism occurred on the erosional platforms of the guyots. This post-erosional activity, represented by the Polar Bear sample dated at 67 Ma, may be related to tectonic activity affecting the plateau and the surrounding plateau margin (Davy et al., 2008). The shallowest ridge-type seamount volcanism may also have formed at similar ages. The similar geochemistry of samples from Kiwi Ridge to samples from the guyot seamounts confirms a similar source for at least the uppermost ridge-type samples. As noted above, the seamount lavas on the Hikurangi Plateau and Kiore Seamount on the adjacent Osbourn ocean crust display distinct geochemical compositions compared to the samples from the Rapuhia Scarp (northern part of the northeast margin where seamount volcanism is absent) and therefore appear to be derived from source material distinct from the plateau basement rocks.

Similar to the Hikurangi Plateau, the Manihiki Plateau is also characterized by the presence of numerous large seamounts. The ~1600 m high Mt. Eddie Seamount and the volcanic base of the Rakahanga Atolls, located between 100 and 140 km northeast of DSDP Site 317 on the High Plateau, were mapped and sampled during the RV Sonne 67-1 cruise (Beiersdorf et al., 1995). Two samples from Mt. Eddie yielded $^{40}Ar/^{39}Ar$ total fusion ages of 75.1 and 81.6 Ma, whereas a volcanic cone north of Mt. Eddie yielded an age of 75.2 Ma (Beiersdorf et al., 1995), consistent with Mt. Eddie having formed well after plateau formation. Similar to the Hikurangi seamount samples, samples from the Manihiki seamounts are highly undersaturated in SiO_2, ranging from nephelinites and basanites to tephrites and hawaiites, and show enrichment in highly to moderately incompatible elements, such as the light REE (Beiersdorf et al., 1995). No published isotopic data are available for Manihiki seamounts; however, Ingle et al. (2007) present geochemical data from several alkalic samples from the Danger Island Troughs. These samples have HIMU-like trace element contents and a Sr–Nd–Pb isotopic composition falling within the range for the Hikurangi seamounts. One of the samples produced an Ar/Ar plateau age of 99.5 ± 0.7 Ma. Although there are no published geochemical data from seamounts and atolls on the Ontong Java Plateau, two alkalic dikes from the Sigana Formation on Isabel Island (Ontong Java Plateau) were dated at ~90 Ma and have HIMU-type trace element and isotopic compositions (Tejada et al., 1996). Therefore, late-stage alkalic magmatism occurred on each of the three plateaus between 99 and 75 Ma. It should be noted that alkaline, HIMU-type seamounts were common in the western Pacific in the Late Cretaceous (e.g. Larson, 1991; Larson and Erba, 1999) and the alkaline volcanism may have been related to a large-scale mantle event. The scarce data from alkalic rocks from Ontong Java and Manihiki, however, suggest that they may be geochemically distinct having lower $^{207}Pb/^{204}Pb$ for a given $^{206}Pb/^{204}Pb$ isotope ratio and higher $^{87}Sr/^{86}Sr$ isotope ratios than the Hikurangi seamount lavas. More data from alkaline rocks, in particular from seamounts, on the Manihiki and Ontong Java Plateaus are needed to evaluate a possible connection between alkalic magmatism on the three plateaus.

As discussed above, the Hikurangi Plateau may have been attached to the Manihiki Plateau (e.g. Billen and Stock, 2000) and possibly also to the Ontong Java Plateau (Taylor, 2006; Worthington et al., 2006; Davy et al., 2008),

but must have been separated from it by 115 Ma ago (Mortimer et al., 2006). The tectonic regime along the West Antarctica–Zealandia part of the Gondwana margin changed from subduction to rifting at 105 ± 5 Ma (Bradshaw, 1989). Therefore the collision of the Hikurangi Plateau with the Gondwana margin (Chatham Rise) may be responsible for the cessation of subduction along the Zealandia part of the Gondwana margin (e.g. Davy and Wood, 1994; Mortimer et al., 2006; Davy et al., 2008). In any case, the Hikurangi Plateau is likely to have been adjacent to Zealandia at the time the HIMU-type seamounts were formed on the plateau. A number of small alkaline igneous complexes in the northeast of the South Island of New Zealand were also formed between 90 and 100 Ma, including the Mandamus (Weaver and Pankhurst, 1991; Tappenden, 2003) and Tapuaenuku (Baker et al., 1994) igneous complexes. Both of these complexes have intraplate (HIMU)-type trace element and Sr–Nd–Pb isotopic compositions (with $^{206}Pb/^{204}Pb$ extending above 20) very similar to those of the Hikurangi Seamounts (see Figs. 7–9). The presence of volcanism with very similar (almost identical) HIMU-type trace element and isotopic characteristics on the Hikurangi Plateau and the South Island of New Zealand provides strong supporting evidence for the arrival of the Hikurangi Plateau at the Gondwana margin by ca. 100 Ma. Late Cretaceous (85–82 Ma) volcanism on the Chatham Islands also has HIMU-like trace element and isotopic compositions similar to that of the Hikurangi seamounts and the ~100–90 Ma South Island volcanism (Panter et al., 2006).

The lack of evidence thus far of HIMU-type compositions in lavas from the Hikurangi Plateau basement and the close similarity in trace element and Sr–Nd–Pb isotopic composition of coeval alkalic volcanism on the plateau and New Zealand suggests that the alkalic seamount volcanism (87–99 Ma) on the Hikurangi Plateau is not derived from the same source as the plateau. Since the lithosphere (crust and mantle) beneath the Hikurangi Plateau should have a composition ranging from MORB to enriched mantle (EM) type Kwaimbaita/Kroenke and Singgalo components, the HIMU-like composition must be coming from a deeper sub-lithospheric source that fed HIMU-like volcanism on both the Zealandia micro-continent and the Hikurangi oceanic plateau.

Several studies have proposed that a HIMU-type plume or plume head was located beneath Marie Byrd Land prior to seperation of Zealandia from West Antarctica and most likely caused this final phase of breakup of Gondwana and controlled the final location of the breakup (e.g. Weaver et al., 1994; Hart et al., 1997; Storey et al., 1999). As noted above, Storey et al. (1999) proposed that the Hikurangi Plateau may have been formed by this HIMU plume event and it appears that at least the seamount volcanism on the plateau may have been. The mid-Cretaceous HIMU-type volcanism on the northern South Island and Chatham Island has also been attributed to this HIMU plume (Weaver et al., 1994; Storey et al., 1999). Mid-Cretaceous (ca. 110–95 Ma) tholeiitic to mildly alkaline mafic dikes and sills from Marie Byrd Land have also been attributed to the same HIMU plume (Weaver et al., 1994; Storey et al., 1999). Although the Pb and Nd isotopic compositions of the Marie Byrd Land dikes are generally less radiogenic and Sr generally more radiogenic than the Hikurangi seamounts and many of the dikes have trace element patterns showing relative Nb and Ta depletion, these geochemical differences could reflect extensive interaction with the thick continental lithosphere beneath the Gondwana core (Weaver and Pankhurst, 1991; Storey et al., 1999).

In conclusion, we propose that both the Hikurangi collision with the Gondwana margin and plume activity beneath Marie Byrd Land could have contributed to the Zealandia–West Antarctica breakup. The Hikurangi collision shut down subduction along the Zealandia part of the Gondwana margin and caused slab detachment. Slab detachment in turn allowed hotter, deeper – in part plume – mantle to upwell first beneath the Chatham Rise and Bounty Trough and subsequently beneath the Campbell Plateau. Southwest propagation of a spreading center on the incoming plate between the western Wishbone and the Bellingshausen Gravity Anomalies may also have contributed to the splitting of Zealandia from West Antarctica (Mortimer et al., 2006).

5.4. Origin of Osbourn seamounts

The geochemistry of the samples from the Osbourn seamounts (located on the abyssal plain adjacent to the Rapuhia Scarp) is distinct from the Hikurangi and Kiore (also on Osbourn seafloor) seamount lavas. They have relatively flat plateau-type trace element patterns on multi-element diagrams that are very similar to those for Kroenke-type lavas from Ontong Java (Fig. 11) with enrichment of Nb and Ta relative to Th and La. The incompatible element abundances, however, are distinctly lower than for Kroenke and even N-MORB-type lavas, except some of the most highly incompatible elements. The isotopic composition is more enriched than 130–170 Ma pre-plateau ocean crust and cannot be explained simply by mixing Kwaimbaita/Kroenke and Singgalo plateau endmembers with depleted upper mantle. The Osbourn isotopic composition, however, lies on an extension of the array formed by the Ontong Java, Manihiki and Hikurangi basement lavas and is similar in composition to lavas from Mauna Kea Volcano, which lies at the end of the Hawaiian array with the highest $^{206}Pb/^{204}Pb$ isotopic composition. The incompatible element patterns and isotopic compositions therefore suggest that Osbourn seamount lavas were derived from a similar source as the plateau basement lavas, but with lower incompatible element concentrations and less radiogenic Sr but more radiogenic Nd, Hf and Pb isotopic compositions.

The Moa (Osbourn) seamount sample is aphyric and has a very low H_2O (0.17) and CO_2 (0.02) contents, suggesting that it is relatively fresh, and thus may represent a primitive melt composition. The major element composition of the Moa sample is similar to a melt derived from mantle peridotite KLB-1 (MG# = 89) at 10 kbar and 1400 °C (Hirose and Kushiro, 1993; KLB-1 run 17), except that total FeO is higher (9 rather than 8 wt%), MgO is lower (14 rather than 16 wt%) and CaO is higher (10 rather than 9 wt%). Derivation from a slightly more fertile peridotite and minor olivine

fractionation could potentially explain these discrepancies. Nevertheless, the incompatible element abundances are not consistent with derivation from melting of an upper mantle MORB or plateau-basement source peridotite. Melting of an already depleted (through previous melt extraction) plateau-basement source should have caused greater relative depletion in the highly to moderately incompatible elements compared to the Kroenke and Kwaimbaita incompatible element patterns on multi-element diagrams. Accumulation of mafic phases such as olivine and pyroxene could cause a uniform dilution of the incompatible elements, however, the Moa sample is aphyric and clearly not a cumulate rock. Near total fusion of an ultramafic cumulate, consisting primarily of olivine and pyroxene, that formed from a primitive plateau-basement melt could explain the similar trace element and isotopic characteristics to Kroenke/Kwaimbaita and Hikurangi lavas and the uniformly lower incompatible element abundances.

The 52 Ma age of the Tuatara (Osbourn) seamount lava indicates that it formed well after the plateau event, which requires a mechanism for bringing cumulate rocks in the plateau root beneath the ocean crust adjacent to the margin. Korenaga (2005) proposed that the 90 Ma old Ontong Java tholeiitic lavas could have formed by pressure-release melting of delaminated pieces of the plateau root that were recirculated (upwelled) by local convective currents caused by the delamination of the root of the plateau. A similar process could be invoked to cause upwelling and melting of delaminated cumulates, derived from the plateau root. Asthenospheric flow against the plateau root could have enhanced local convective currents at the plateau margin. Interestingly, the isotopic composition of the Osbourn seamounts may reflect a plateau endmember composition, similar to the isotopic composition of Mauna Kea, Hawaii lavas, representing one of the endmembers for Hawaiian shield volcanoes.

6. CONCLUSIONS

Three different morphological units on and near the Hikurangi Plateau were mapped and sampled during Sonne cruise 168: (1) basement exposed at the northernmost part of the northeastern plateau margin (Rapuhia Scarp), interpreted to be a rifted margin, (2) large guyot and ridge-type seamounts on the plateau, and (3) seamounts on the abyssal plain adjacent to the Rapuhia Scarp. Feldspars from plateau basement samples produced mean apparent $^{40}Ar/^{39}Ar$ ages of 118–96 Ma, whereas feldspar, hornblende and matrix step-heating analyses of the plateau seamounts yielded ages of 99–87 and 67 Ma. An age of 52 Ma was obtained from a sample from one of the abyssal Osbourn seamounts. Ages determined on two DSDP Site 317 samples (116–117 Ma) are similar to the oldest age from the Hikurangi basement.

The three morphological units also display distinct geochemical compositions. The Hikurangi and Manihiki basement samples have tholeiitic geochemical affinities and have flat immobile incompatible element patterns on primitive-mantle-normalized multi-element diagrams. The incompatible element and isotope data for the Hikurangi basement indicate that the plateau basement was largely derived from an enriched EM-type source very similar to Kwaimbaita rocks from the Ontong Java Plateau. Samples from DSDP Site 317 and possibly a single sample from the Hikurangi basement have similar, although distinct in detail, incompatible element and isotopic compositions to the more EM1-type Singgalo lavas from Ontong Java. Therefore the available age and geochemical data from the Hikurangi and Manihiki Plateaus support derivation of these plateaus from the Greater Ontong Java Event. We propose that a secondary plume swarm from a superplume head or dome stalled at the transition zone could explain the Greater Ontong Java Event.

Samples from Osbourn seamounts on the abyssal plain adjacent to the Rapuhia Scarp have incompatible element characteristics similar to Kroenke lavas from the Ontong Java Plateau, but lower absolute abundances. The isotope data fall on an extension of the array formed by the Ontong Java, Hikurangi and Manihiki plateaus. Taken together the trace element and isotope data suggest derivation through melting of ultramafic cumulates derived from the plateau root. Local convective currents could cause upwelling and decompression melting of some detached portions of the plateau root.

The Hikurangi seamount lavas are alkalic and show enrichment in highly to moderately incompatible elements (e.g. Th, Nb, Ta, LREE, Zr, Hf, Pb) relative to less incompatible elements (e.g. heavy REE, Y). The seamount samples also have more radiogenic Pb and less radiogenic Sr, Nd and Hf isotope ratios than the plateau lavas. The Hikurangi seamount lavas are derived from a HIMU OIB-type mantle source similar to contemporaneous volcanism on Zealandia and on Marie Byrd Land Antarctica, which was attached to Zealandia in the mid-Cretaceous. We suggest that this volcanism was related to a mid-Cretaceous plume event that may have contributed to the final breakup phase of Gondwana.

ACKNOWLEDGEMENTS

We thank Captain Kull, ship's crew and scientific party for contributing to the great success of the SO168 cruise. S. Hauff, D. Rau and J. Sticklus are thanked for technical assistance. GNS provided maps, data and invaluable information that helped make the cruise a success. The Integrated Ocean Drilling Program (IODP) is acknowledged for providing DSDP Site 317 samples. Discussions with R. Herzer, C. Timm, J. Phipps-Morgan, M. Portnyagin and C. Herzberg helped develop ideas in this paper. We are grateful to M. Großman and M. Tormann for help with processing of the SIMRAD data and to A. Brandon, M. Tejeda and two anonymous reviewers for their constructive comments that helped improve the manuscript. The German Ministry of Education and Research (BMBF; Grants SO168 ZEALANDIA and SO193 MANIHIKI) funded this research.

APPENDIX A. SUPPLEMENTARY DATA

Supplementary data associated with this article (EA1 - Ar/Ar age dating methods, EA2 - Ar/Ar single analyses, and EA3 - major and trace element data) can be found, in the online version, at doi:10.1016/j.gca.2010.09.030.

REFERENCES

Abouchami W., Hofmann A. W., Galer S. J. G., Frey F. A., Eisele J. and Feigenson M. (2005) Lead isotopes reveal bilateral asymmetry and vertical continuity in the Hawaiian mantle plume. *Nature* **434**, 851–856.

Anderson D. L., Zhang Y.-S. and Tanimoto T. (1992) Plume heads, continental lithosphere, flood basalts and tomography. In *Magmatism and the Causes of Continental Break-up* (eds. B. C. Storey, T. Alabaster and R. J. Pankhurst). *Geological Society Special Publication* **68**, pp. 99–124.

Baker J. A., Gamble J. A. and Graham I. J. (1994) The age, geology and geochemistry of the Tapuaenuku Igneous Complex, Marlborough, New Zealand. *NZ J. Geol. Geophys.* **37**, 249–268.

Baker J. A., Peate D. W., Waight T. E. and Thirlwall M. F. (2005) Reply to the: comment on "Pb isotopic analysis of standards and samples using a 207Pb–204Pb double spike and thallium to correct for mass bias with a double focusing MC-ICP-MS" by Baker et al.. *Chem. Geol.* **217**, 175–179.

Baksi A. K. (2003) Critical evaluation of 40Ar/39Ar ages from the Central Atlantic Magmatic Province: timing, duration and possible migration of magmatic centers. In *The Central Atlantic Magmatic Province, Insights from Pangaea; AGU Monograph* **136** (eds. W. Hames, J. G. McHone, P. R. Renne and C. Ruppel), pp. 77–90.

Baksi A. K. (2005) Evaluation of radiometric ages pertaining to rocks hypothesized to have been derived by hotspot activity, in and around the Atlantic, Indian, and Pacific Oceans. *GSA Spec. Pap.* **388**, 55–70.

Beiersdorf H., Bach W., Duncan R. A., Erzinger J. and Weiss W. (1995) New evidence for the production of EM-type ocean island basalts and large volumes of volcaniclastites during the early history of the Manihiki Plateau. *Mar. Geol.* **122**, 181–205.

Beiersdorf H. and Erzinger J. (1989) Observations on the bathymetry and geology of the northeastern Manihiki Plateau, southwest Pacific Ocean. *S. Pac. Mar. Geol. Notes* **4**, 33–46.

Billen M. I. and Stock J. (2000) Morphology and origin of the Osbourn Trough. *J. Geophys. Res.* **105**, 13481–13489.

Blichert-Toft J., Chauvel C. and Albarede F. (1997) Separation of Hf and Lu for high-precision isotope analyses of rock samples by magnetic sector-multiple collector ICP-MS. *Contrib. Mineral. Petrol.* **127**, 248–260.

Bogaard P. v. d. (1995) 40Ar/39Ar ages of sanidine phenocrysts from Laacher See Tephra (12,900 yr BP): chronostratigraphic and petrological significance. *Earth Planet. Sci. Lett.* **133**, 163–174.

Bogaard P. v. d., Hall C. M., Schmincke H.-U. and York D. (1987) 40Ar/39Ar laser dating of single grains: ages of Quaternary Tephra from the East Eifel Volcanic Field. *Geophys. Res. Lett.* **14**, 1211–1214.

Bogaard P. v. d., Hall C. M., Schmincke H.-U. and York D. (1989) Precise single-grain 40Ar/39Ar dating of a cold to warm climate transition in Central Europe. *Nature* **342**, 523–525.

Bradshaw J. D. (1989) Cretaceous geotectonic patterns in the New Zealand region. *Tectonics* **8**, 803–820.

Bukry D. (1976) Coccolith Stratigraphy of Manihiki Plateau, Central Pacific, Deep Sea Drilling Project, Site 317. In *Initial Reports of the Deep Sea Drilling Project*, vol. 33 (eds. S. O. Schlanger and E. D. Jackson). U.S. Government Printing Office, Washington, DC, pp. 493–501.

Chambers L. M., Pringle M. S. and Fitton J. G. (2002) Age and duration of magmatism on the Ontong Java Plateau: 40Ar–39Ar results from ODP Leg 192. *Eos, Trans. Am. Geophys. Union, 83* (*Suppl.*) *Abstract V71B-1271.*

Clague D. A. (1976) Petrology of basaltic and gabbroic rocks dredged from the Danger Island Troughs, Manihiki Plateau. In *Initial Reports of the Deep Sea Drilling Project*, vol. 33 (eds. S. O. Schlanger and E. D. Jackson). U.S. Government Printing Office, Washington, DC, pp. 891–911.

Coffin M. F. and Eldholm O. (1993) Scratching the surface: estimating dimensions of large igneous provinces. *Geology* **21**, 515–518.

Coffin M. F. and Eldholm O. (1994) Large igneous provinces: crustal structure, dimensions, and external consequences. *Rev. Geophys.* **32**, 1–36.

Courtillot V., Davaille A., Besse J. and Stock J. (2003) Three distinct types of hotspots in the Earth's mantle. *Earth Planet. Sci. Lett.* **205**, 295–308.

Davaille A., Girard F. and Le Bars M. (2002) How to anchor hotspots in a convecting mantle? *Earth Planet. Sci. Lett.* **203**, 621–634.

Davy B., Hoernle K. and Werner R. (2008) Hikurangi Plateau: crustal structure, rifted formation, and Gondwana subduction history. *Geochem. Geophys. Geosyst.* **9**, Q07004. doi:10.1029/2007GC001855.

Davy B. and Wood R. (1994) Gravity and magnetic modelling of the Hikurangi Plateau. *Mar. Geol.* **118**, 139–151.

Farley K. A. and Neroda E. (1998) Noble gases in the Earth's mantle. *Annu. Rev. Earth Planet. Sci.* **26**, 189–218.

Farnetani C. G. and Samuel H. (2005) Beyond the thermal plume paradigm. *Geophys. Res. Lett.* **32**, L07311. doi:10.1029/2005GL022360.

Fitton J. G. and Godard M. (2004) Origin and evolution of magmas on the Ontong Java Plateau. In *Origin and Evolution of the Ontong Java Plateau* (eds. J. G. Fitton, J. J. Mahoney, P. J. Wallace and A. D. Saunders). *Geological Society London Special Publication* **229**, London, pp. 151–178.

Fitton J. G., Mahoney J. J., Wallace P. J. and Saunders A. D. (2004) Origin and evolution of the Ontong Java Plateau: introduction. In *Origin and Evolution of the Ontong Java Plateau* (eds. J. G. Fitton, J. J. Mahoney, P. J. Wallace and A. D. Saunders). *Geological Society London Special Publication* **229**, London, pp. 1–8.

Galer S. J. G. and Abouchami W. (1998) Practical application of lead triple spiking triple spiking for correction of instrumental mass discrimination. *Mineral. Mag.* **62A**, 491–492.

Gansecki C. A. and Mahood G. A. (1998) New ages for the climactic eruptions at Yellowstone: single-crystal 40Ar/39Ar dating identifies contamination. *Geology* **26**, 343–346.

Garbe-Schönberg C.-D. (1993) Simultaneous determination of thirty-seven trace elements in twenty-eight international rock standards by ICP-MS. *Geostand. Newsl.* **17**, 81–97.

Geldmacher J., Hoernle K., Klügel A., Bogaard P. v. d., Wombacher F. and Berning B. (2006) Origin and geochemical evolution of the Madeira-Tore Rise (eastern North Atlantic). *J. Geophys. Res.* **111**, B09206. doi:10.1029/2005JB003931.

Giaccio B., Marra F., Hajdas I., Karner D. B., Renne P. R. and Sposato A. (2009) 40Ar/39Ar and 14C geochronology of the Albano maar deposits: implications for defining the age and eruptive style of the most recent explosive activity at Colli Albani Volcanic District, Central Italy. *J. Volcanol. Geotherm. Res.* **185**, 203–213.

Gladczenko T. Z., Coffin M. F. and Eldholm O. (1997) Crustal structure of the Ontong Java Plateau: modelling of new gravity and existing seismic data. *J. Geophys. Res.* **102**, 22711–22729.

Gradstein F. M., Agterberg F. P., Ogg J. G., Hardenbol J., van Veen P., Thierry J. and Huang Z. (1994) A mesozoic time scale. *J. Geophys. Res.* **99**, 24051–24074.

Hart S. R., Blusztajn J., LeMasurier W. E. and Rex D. C. (1997) Hobbs Coast Cenozoic volcanism: implications for the West Antarctic rift system. *Chem. Geol.* **139**, 223–248.

Hauff F., Hoernle K. and Schmidt A. (2003) The Sr–Nd–Pb composition of Mesozoic Pacific ocean crust (Site 1149 and 801, ODP Leg 185): implications for alteration of ocean crust and the input into the Izu-Bonnin-Marina subduction system. *Geochem. Geophys. Geosyst.* **4**, 8913. doi:10.1029/2002GC000421.

Herzberg C. (2004) Partial melting below the Ontong Java Plateau, in origin and evolution of the Ontong Java Plateau. In *Origin and Evolution of the Ontong Java Plateau* (eds. J. G. Fitton, J. J. Mahoney, P. J. Wallace and A. D. Saunders). *Geological Society London Special Publication* **229**, London, pp. 179–183.

Herzberg C., Asimow P. D., Arndt N., Niu Y., Lesher C. M., Fitton J. G., Cheadle M. J. and Saunders A. D. (2007) Temperatures in ambient mantle and plumes: constraints from basalts, picrites, and komatiites. *Geochem. Geophys. Geosyst.* **8**, Q02006. doi:10.1029/2006GC001390.

Hirose K. and Kushiro I. (1993) Partial melting of dry peridotites at high pressures: determination of compositions of melts segregated from peridotite using aggregates of diamond. *Earth Planet. Sci. Lett.* **114**, 477–489.

Hoernle K., Hauff F., Werner R. and Mortimer N. (2004) New insights into the origin and evolution of the Hikurangi oceanic plateau. *EOS Transactions AGU* **85**, 401, 408.

Hoernle K., Hauff F., Werner R., van den Bogaard P., Timm C., Coffin M., Mortimer N. and Davy B. (2008) A similar multi-stage geochemical evolution for the Manihiki, Hikurangi and Ontong Java Plateaus? *AGU Fall Meeting, San Fransisco, USA, December 14–19, Eos Trans. AGU, 89(53), Fall Meet. Suppl., Abstract V23H-05.*

Hoernle K., Mortimer N., Werner R. and Hauff F. (2003) Cruise Report SO168 (ZEALANDIA): causes and effects of plume and rift related Cretaceous and Cenozoic volcanism on Zealandia. *GEOMAR Rep.* **113**, 1–127.

Hoernle K., Timm C., Hauff F., Rupke L., Werner R., Bogaard P. v. d., Michael P. J., Coffin M., Mortimer N. N. and Davy, B. W. (2009) New results for the multi-stage geochemical evolution of the Manihiki and Hikurangi Plateaus. *AGU Fall Meeting, San Fransisco, USA, December 14–18, Eos Trans. AGU, 90 (53), Fall Meet. Suppl., Abstract V51H-03, Invited Talk.*

Hoernle K. A. and Tilton G. R. (1991) Sr–Nd–Pb isotope data for Fuerteventura (Canary Islands) basal complex and subaerial volcanics: applications to magma genesis and evolution. *Schweiz. Mineral. Petrogr. Mitt.* **71**, 3–18.

Ingle S. and Coffin M. F. (2004) Impact origin for the greater Ontong Java Plateau? *Earth Planet. Sci. Lett.* **218**, 123–134.

Ingle S., Mahoney J. J., Sato H., Coffin M. F., Kimura J.-I., Hirano N. and Nakanishi M. (2007) Depleted mantle wedge and sediment fingerprint in unusual basalts from the Manihiki Plateau, central Pacific Ocean. *Geology* **35**, 595–598.

Ishikawa A., Maruyama S. and Komiya T. (2004) Layered Lithospheric Mantle Beneath the Ontong Java Plateau: implications from Xenoliths in Alnoite, Malaita, Solomon Islands. *J. Petrol.* **45**, 2011–2044.

Ito G. and Clift P. D. (1998) Subsidence and growth of Pacific Cretaceous plateaus. *Earth Planet. Sci. Lett.* **161**, 85–100.

Jackson E. D., Bargar K. E., Fabbi B. P. and Heropoulos C. (1976) Petrology of the basaltic rocks drilled on Leg 33 of the Deep Sea Drilling Project. In *Initial Reports of the Deep Sea Drilling Project*, vol. 33 (eds. S. O. Schlanger and E. D. Jackson). U.S. Government Printing Office, Washington, DC, pp. 571–630.

Janney P. E. and Castillo P. R. (1997) Geochemistry of Mesozoic Pacific mid-ocean ridge basalt: constraints on melt generation and the evolution of the Pacific upper mantle. *J. Geophys. Res.* **102**, 5207–5229.

Korenaga J. (2005) Why did not the Ontong Java Plateau form subaerially? *Earth Planet. Sci. Lett.* **234**, 385–399.

Kurz M. D., Jenkins W. J., Hart S. R. and Clague D. (1983) Helium isotopic variations in volcanic rocks from Loihi Seamount and the Island of Hawaii. *Earth Planet. Sci. Lett.* **66**, 388–406.

Larson R. L. (1991) Geological consequences of superplumes. *Geology* **19**, 963–966.

Larson R. L. and Erba E. (1999) Onset of the mid-Cretaceous greenhouse in the Barremian–Aptian: igneous events and the biological, sedimentary, and geochemical responses. *Paleoceanography* **14**, 663–678.

Larson R. L., Pockalny R. A., Viso R. F., Erba E., Abrams L. J., Luyendyk B. P., Stock J. M. and Clayton R. W. (2002) Mid-Cretaceous tectonic evolution of the Tongareva triple junction in the southwestern Pacific Basin. *Geology* **30**, 67–70.

Lewis K. B. and Bennett D. J. (1985) Structural patterns on the Hikurangi Margin: and interpretation of new seismic data. *NZ Oceanogr. Field Rep.* **22**, 3–25.

Ludwig K. R. (2003) Isoplot 3.00 – a geochronological toolkit for Microsoft Excel. *Berkeley Geochronol. Cent. Spec. Publ.* **4**, 1–70.

Mahoney J. J. (1987) An isotopic survey of Pacific oceanic plateaus: implications for their nature and origin. In *Seamounts, Islands, and Atolls* (eds. B. H. Keating, P. Fryer, R. Batiza and G. W. Boehlert). *American Geophysical Union Monograph* **43**, Washington, DC, pp. 207–220.

Mahoney J. J., Frei R., Tejada M. L. G., Mo X. X., Leat P. T. and Nägler T. F. (1998) Tracing the Indian Ocean mantle Domain through time: isotopic results from old West Indian, East Tethyan, and South Pacific seafloor. *J. Petrol.* **39**, 1285–1306.

Mahoney J. J. and Spencer K. J. (1991) Isotopic evidence for the origin of the Manihiki and Ontong Java oceanic plateaus. *Earth Planet. Sci. Lett.* **104**, 196–210.

Mahoney J. J., Storey M., Duncan R. A., Spencer K. J. and Pringle M. (1993) Geochemistry and age of the Ontong Java Plateau. In *The Mesozoic Pacific: Geology, Tectonics and Volcanism* (eds. M. S. Pringle, W. W. Sager, W. V. Sliter and S. Stein). Geophysical Monograph, vol. 77. American Geophysical Union, Washington, pp. 233–261.

McNulty C. L. (1976) Cretaceous foraminiferal stratigraphy, DSDP Leg 33, Hole 315A, 316, 317A. In *Initial Reports of the Deep Sea Drilling Project*, vol. 33 (eds. S. O. Schlanger and E. D. Jackson). U.S. Government Printing Office, Washington, DC, pp. 369–381.

Montelli R., Nolet G., Dahlen F. A. and Masters G. (2006) A catalogue of deep mantle plumes: new results from finite-frequency tomography. *Geochem. Geophys. Geosyst.* **7**, Q11007. doi:10.1029/2006GC001248.

Montelli R., Nolet G., Dahlen F. A., Masters G., Engdahl E. R. and Hung S.-H. (2004) Finite-frequency tomography reveals a variety of plumes in the mantle. *Science* **303**, 338–343.

Mortimer N., Hoernle K., Hauff F., Palin J. M., Dunlap W. J., Werner R. and Faure K. (2006) New constraints on the age and evolution of the Wishbone Ridge, southwest Pacific Cretaceous microplates, and Zealandia–West Antarctica breakup. *Geology* **34**, 185–188.

Mortimer N. and Parkinson D. (1996) Hikurangi Plateau: a Cretaceous large igneous province in the southwest Pacific Ocean. *J. Geophys. Res.* **101**, 687–696.

Neal C. R., Mahoney J. J., Kroenke L. W., Duncan R. A. and Petterson M. G. (1997) The Ontong Java Plateau. In *Large Igneous Provinces* (eds. J. J. Mahoney and M. F. Coffin). *American Geophysical Union Monograph* **100**, Washington, pp. 183–216.

Panter K. S., Blusztajn J., Hart S. R., Kyle P. R., Esser R. and McIntosh W. C. (2006) The origin of HIMU in the SW Pacific: evidence from Intraplate Volcanism in Southern New Zealand and Subantarctic Islands. *J. Petrol.* **47**, 1673–1704.

Reyners M. et al. (2006) Imaging subduction from the trench to 300 km depth beneath the central North Island, New Zealand, with Vp and Vp/Vs. *Geophys. J. Int.* **165**, 565–583.

Richardson W. P., Okal E. A. and Van der Lee S. (2000) Rayleigh-wave tomography of the Ontong-Java Plateau. *Phys. Earth Planet. Inter.* **118**, 29–51.

Roberge J., Wallace P. J., White R. V. and Coffin M. F. (2005) Anomalous uplift and subsidence of the Ontong Java Plateau inferred from CO_2 contents of submarine basaltic glasses. *Geology* **33**, 501–504.

Roberge J., White R. V. and Wallace P. J. (2004) Volatiles in basaltic magmas from the Ontong Java Plateau: implications for magmatic processes and source region compositions. In *Origin and Evolution of the Ontong Java Plateau* (eds. J. G. Fitton, J. J. Mahoney, P. J. Wallace and A. D. Saunders). *Geological Society London Special Publication* **229**, London, pp. 239–257.

Rogers G. C. (1982) Oceanic plateaus as meteorite impact signatures. *Nature* **299**, 341–342.

Schlanger S. O., Jackson E. D., Boyce R. E., Cook H. E., Jenkyns H. C., Johnson D. A., Kaneps A. G., Kelts K. R., Martini E., McNulty C. L. and Winterer E. L. (1976) *Initial Reports of the Deep Sea Drilling Project 33*. US Government Printing Office, Washington, pp. 967.

Shervais J. W. (1982) Ti–V plots and the petrogenesis of modern and ophiolitic lavas. *Earth Planet. Sci. Lett.* **59**, 101–118.

Sikora P. J. and Bergen J. A. (2004) Lower Cretaceous planktonic foraminiferal and nannofossil biostratigraphy of Ontong Java Plateau sites from DSDP Leg 30 and ODP Leg 192. In *Origin and Evolution of the Ontong Java Plateau* (eds. J. G. Fitton, J. J. Mahoney, P. J. Wallace and A. D. Saunders). *Geological Society London Special Publication* **229**, London, pp. 83–111.

Sliter W. V. (1992) Cretaceous planktic foraminiferal biostratigraphy and paleoceanography recents in the Pacific Ocean with emphasis on indurated sediment. In *Centenary of Japanese Micropaleontology* (eds. K. Ishizaki and T. Saito). Terra Scientific Publishing, Tokyo, Japan., pp. 281–299.

Storey B. C., Leat P. T., Weaver S. D., Pankhurst R. J., Bradshaw J. D. and Kelley S. (1999) Mantle plumes and Antarctica–New Zealand rifting: evidence from mid-Cretaceous mafic dykes. *J. Geol. Soc. Lond.* **156**, 659–671.

Strong C. P. (1994) Late Cretaceous foraminifera from Hikurangi Plateau, New Zealand. *Mar. Geol.* **119**, 1–5.

Suetsugu D., Isse T., Tanaka S., Obayashi M., Shiobara H., Sugioka H., Kanazawa T., Fukao Y., Barruol G. and Reymond D. (2009) South Pacific mantle plumes imaged by seismic observation on islands and seafloor. *Geochem. Geophys. Geosyst.* **10**, Q11014. doi:10.1029/2009GC002533.

Sun S.-S. and McDonough W. F. (1989) Chemical and isotopic systematics of oceanic basalts: implications for mantle composition and processes. In *Magmatism in the Ocean Basins*, vol. 42 (eds. A. D. Saunders and M. J. Norry). Geological Society London, Special Publication, London, pp. 313–345.

Tappenden V. E. (2003) Magmatic response to the evolving New Zealand margin of Gondwana during the Mid-Late Cretaceous. Ph.D. Thesis, University of Canterbury, Christchurch, New Zealand.

Tarduno J. A., Sliter W. F., Leckie M., Mayer H., Mahoney J. J., Musgrave R., Storey M. and Winterer E. L. (1991) Rapid formation of Ontong Java plateau by Aptian mantle plume volcanism. *Science* **254**, 399–403.

Taylor B. (2006) The single largest oceanic plateau: Ontong Java-Manihiki-Hikurangi. *Earth Planet. Sci. Lett.* **241**, 372–380.

Tejada M. L. G., Mahoney J. J., Castillo P. R., Ingle S. P., Sheth H. C. and Weis D. (2004) Pin-picking the elephant: evidence on the origin of the Ontong Java Plateau from Pb–Sr–Hf–Nd isotopic characteristics of ODP Leg 192 basalts. In *Origin and Evolution of the Ontong Java Plateau* (eds. J. G. Fitton, J. J. Mahoney, P. J. Wallace and A. D. Saunders). *Geological Society London Special Publication* **229**, London, pp. 133–150.

Tejada M. L. G., Mahoney J. J., Duncan R. A. and Hawkins M. P. (1996) Age and geochemistry of basement and alkalic rocks of Malaita and Santa Isabel, Soloman Islands, southern margin of Ontong Java Plateau. *J. Petrol.* **37**, 361–394.

Tejada M. L. G., Mahoney J. J., Neal C. R., Duncan R. A. and Petterson M. G. (2002) Basement geochemistry and geochronology of Central Malaita, Solomon Islands, with implications for the origin and evolution of the Ontong Java Plateau. *J. Petrol.* **43**, 449–484.

Thirlwall M. F. (2000) Inter-laboratory and other errors in Pb isotope analyses investigated using a ^{207}Pb–^{204}Pb double spike. *Chem. Geol.* **163**, 299–322.

Thirlwall M. F. (2002) Multicollector ICP-MS analysis of Pb isotopes using a ^{207}Pb–^{204}Pb double spike demonstrates up to 400 ppm/amu systematic errors in Tl-normalization. *Chem. Geol.* **184**, 255–279.

Thordason T. (2004) Accretionary-lapilli-bearing pyroclastic rocks at ODP Leg 192 Site 1184: a record of subaerial phreatomagmatic eruptions on the Ontong Java Plateau. In *Origin and Evolution of the Ontong Java Plateau* (eds. J. G. Fitton, J. J. Mahoney, P. J. Wallace and A. D. Saunders). *Geological Society London Special Publication* **229**, London, pp. 275–306.

Viso R. F., Larson R. L. and Pockalny R. A. (2005) Tectonic evolution of the Pacific-Phoenix-Farallon triple junction in the South Pacific Ocean. *Earth Planet. Sci. Lett.* **233**, 179–194.

Weaver S. D. and Pankhurst R. J. (1991) A precise Rb–Sr age for the Mandamus Igneous Complex, North Canterbury, and regional tectonic implications. *NZ J. Geol. Geophys.* **34**, 341–345.

Weaver S. D., Storey B. C., Pankhurst R. J., Mukasa S. B., DiVenere V. J. and Bradshaw J. D. (1994) Antarctica–New Zealand rifting and Marie Byrd Land lithospheric magmatism linked to ridge subduction and mantle plume activity. *Geology* **22**, 811–814.

Wolfe C. J., Solomon S. C., Laske G., Collins J. A., Detrick R. S., Orcutt J. A., Bercovici D. and Hauri E. H. (2009) Mantle shear-wave velocity structure beneath the Hawaiian Hot Spot. *Science* **326**, 1388–1390.

Wood R. and Davy B. (1994) The Hikurangi Plateau. *Mar. Geol.* **118**, 153–173.

Worthington T. J., Hekinian R., Stoffers P., Kuhn T. and Hauff F. (2006) Osbourn Trough: structure, geochemistry and implications of a mid-Cretaceous paleospreading ridge in the South Pacific. *Earth Planet. Sci. Lett.* **245**, 685–701.

York D. (1969) Least squares fitting of a straight line with correlated errors. *Earth Planet. Sci. Lett.* **5**, 320–324.

Zindler A. and Hart S. (1986) Chemical geodynamics. *Ann. Rev. Earth Planet. Sci. Lett.* **14**, 493–571.

Associate editor: Alan D. Brandon